AD-A270 424

REPORT DATE	3. REPORT TYPE AND DATES COVERED
	FINAL TECHNICAL 2/1/90-3/31/93

4. TITLE AND SUBTITLE
KINETIC ASPECTS OF LATTICE MISMATCH IN MOLECULAR BEAM EPITAXICAL GROWTH ON PLANAR AND PATTERNED SUBSTRATES

5. FUNDING NUMBERS
AFOSR-90-0184

6. AUTHOR(S)
A. MADHUKAR

7. PERFORMING ORGANIZATION NAME(S) AND ADDRESS(ES)
UNIVERSITY OF SOUTHERN CALIFORNIA
DEPARTMENT OF MATERIALS SCIENCE AND ENGINEERING
SCHOOL OF ENGINEERING
LOS ANGELES, CA 90089-0241

8. PERFORMING ORGANIZATION REPORT NUMBER
AFOSR-TR- 93 0744

9. SPONSORING/MONITORING AGENCY NAME(S) AND ADDRESS(ES)
AIR FORCE OFFICE OF SCIENTIFIC RESEARCH
ELECTRONIC AND MATERIALS SCIENCES DIRECTORATE
BOLLING AIR FORCE BASE
WASHINGTON, DC 20322

10. SPONSORING/MONITORING AGENCY REPORT NUMBER
2305/B1

11. SUPPLEMENTARY NOTES

12a. DISTRIBUTION/AVAILABILITY STATEMENT
APPROVED FOR PUBLIC RELEASE
DISTRIBUTION UNLIMITED

12b. DISTRIBUTION CODE

13. ABSTRACT (Maximum 200 words)

This final scientific report summarizes the salient accomplishments under the grant AFOSR 90-0184 which include (i) the first demonstration of the realization of 3-dimensionally confined (i.e. quantum box) GaAs structures via a one-step MBE growth on pre-patterned nonplanar GaAs(111)B and GaAs(100) substrates and exhibiting optical activity, (ii) the first demonstration of the kinetics of highly strained InGaAs 3D island and defect formation and the potential use of such coherent islands as quantum boxes, (iii) introduction of the idea of substrate encoded size-reducing epitaxy (SESRE) that underlies (i) above and provides a means for exploiting (ii) for the creation of a regular array of coherent 3D InAs islands as a quantum box array, (iv) realization of high quality, highly strained GaAs/InGaAs/AlGaAs single and multiple quantum well structures via RHEED optimized growth kinetics control and their application to high performance resonant tunnelling diodes, doped-channel MISFETs, and asymmetric Fabry-Perot spatial light modulators in a novel inverted cavity geometry, (v) the impact of *ex-situ* processing steps such as dielectric encapsultation and rapid thermal annealing, and (vi) the use of Ga^+ focused ion beam for *in-situ* direct-write patterning of GaAs.

14. SUBJECT TERMS GaAs(111)B/AlGaAs HETEROEPITAXY, PRE-PATTERNED GROWTH 3-D CONFINED NANOSTRUCTURES, GaAs(100)/InGaAs/AlGaAs HIGHLY STRAINED QUANTUM WELLS, Si_3N_4 ENCAPSULATION, RAPID THERMAL ANNEALING, Ga FOCUSSED ION BEAM PATTERNING.

15. NUMBER OF PAGES

16. PRICE CODE

17. SECURITY CLASSIFICATION OF REPORT	18. SECURITY CLASSIFICATION OF THIS PAGE	19. SECURITY CLASSIFICATION OF ABSTRACT	20. LIMITATION OF ABSTRACT
UNCLASSIFIED	UNCLASSIFIED	UNCLASSIFIED	UL

FINAL SCIENTIFIC REPORT

AFOSR GRANT NO. AFOSR-90-0184

PERIOD: FEB. 01, 1990 TO MAR. 31, 1993

KINETIC ASPECTS OF LATTICE MISMATCH IN MOLECULAR BEAM EPITAXICAL GROWTH ON PLANAR AND PATTERNED SUBSTRATES

Submitted to

AIR FORCE OFFICE OF SCIENTIFIC RESEARCH
ELECTRONIC & MATERIALS SCIENCES DIRECTORATE
AFOSR/NE
110 DUNCAN AVENUE, SUITE B115
BOLLING AIR FORCE BASE
WASHINGTON, D.C. 20332-0001

ATTN: LT. COL. GERNOT S. POMRENKE

Submitted by

ANUPAM MADHUKAR
DEPT. OF MATERIALS SCIENCE & ENG.
UNIVERSITY OF SOUTHERN CALIFORNIA
LOS ANGELES, CA 90089-0241

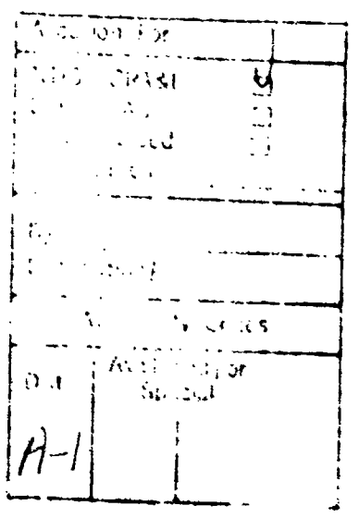

CONTENTS

Abstract

In this Final Scientific Report on grant number AFOSR-90-0184 we summarize the highlights of the work accomplished under this support. The work has covered six different though inter-related areas and resulted in nearly sixty publications involving five graduate students. The six areas are detailed in the attached list. Several new ideas and novel approaches addressing (i) ways of examining the nature of the atomisitic surface kinetics during molecular beam epitaxical growth of lattice matched ($GaAs/Al_xGa_{1-x}As$) and strained ($GaAs/In_xGa_{1-x}As$) systems and (ii) exploiting these for (a) creation of 3-dimensionally confined nanostructures (i.e. quantum dots) and (b) reduction in defect density, both via growth on prepatterned substrates, have been introduced and successfully demonstrated. The major highlights of the accomplishments are;

1. First demonstration of the realization of twin-free and mirror smooth surfaces in $GaAs(111)B/Al_xGa_{1-x}As$ MBE growth on non-miscut (i.e. singular) GaAs(111)B substrates. (See sec. I.1)

2. The first realization of 3-dimensionally confined structures via a one-step *in-situ* growth process on triangular base mesas on GaAs(111)B and square base mesas on GaAs(100). Structures with lateral linear dimensions <500°A and as small as 325°A have been realized as seen in cross-sectional high resolution electron microscope studies and their optical activity (luminescence) demonstrated via spectrally- and spatially-resolved cathodoluminescence studies. (See sec. I.5)

3. An explanation of the directionality of interfacet migration observed in all studies for nearly a decade was provided for the first time. It is based upon the role of step-step interaction on the sidefacets of a patterned mesa arising from the interaction of the stress fields. This led us to introduce the concept of substrate-encoded size-reducing epitaxy (SESRE) that, in fact, forms the conceptual basis for the realization of the quantum dot structures noted under point 2 above. (See sec. I.5)

4. The first study of the formation kinetics of strained 3D InGaAs islands on GaAs(100) and their possible use as 3-dimensionally confined quantum dot sturctures, placed in a regular array via the use of deposition on pre-patterned mesas. This study has revealed that the 3D island formaton kinetics, and hence the island size distribution and the demarcation lie between coherent and incoherent islands as a function of the island size, is not controlled by simply III surface diffusion kinetics as has been explicitly or implicitly assumed hitherto in all considerations of island formation. Rather, the strain-dependent group V and III incorporation kinetics at the growing island edges and the kinetics of new island initiation play a significant competing role with the surface diffusion kinetics. Optimized growth conditions for achieving the desired island size distribution with nearly exclusively coherent islands of lateral size <400°A have been obtained. (See sec. I.2)

5. Optimized growth kinetics for the realization of highly strained (~2%) high In and Al content GaAs/$Al_yGa_{1-y}As$/$In_xGa_{1-x}As$/$Al_zGa_{1-z}As$ symmetric (y=z) and asymmetric (y≠z) single and thick multiple quantum wells have been achieved using reflection high-energy electron diffraction as an *in-situ* diagnostic tool. Using these optimized growth conditions, the highest quality wells for applications in (a) highly strained resonant tunnelling diodes, (b) pseudomorphic HEMTs and doped-channel MISFETs, and (c) asymmetric Fabry-Perot spatial light modulators for digital (optical switches) and analog (neural network) applications have been succesfully realized and high quality device performance demonstrated. (See sec. I.3)

6. The effect of the two of the more common processing steps towards device completion, i.e. dielectric encapsulation and rapid thermal annealing (RTA), on the structural and optical quality of the as-grown highly strained InGaAs/AlGaAs quantum well structures was examined systematically, including theoretical modeling of the interfacial inter-diffusion process. Blue shifts in the exciton line were seen to be introduced by Si_3N_4 encapsulation and by RTA, less so by the former alone. Dielectric encapsulated specimens show less degradation with RTA than unencapsulated specimens. (See sec. I. 4)

7. A final subject on which work was initiated pertains to Ga+ focused ion beam (FIB) assisted direct-write and in-situ patterning of GaAs(100). Monies for the acquistion of some of the instrumentation needed for this work were provided as supplemental capital equipment funds. During the period of this contract work was undertaken on the issue of Ga droplet formation in direct sputtering of GaAs. Studies have led to the first determination of the Ga+ dose threshold for the formation of the Ga droplet, determination of the surface stoichiometry, and a mechanism for the formation of the droplets. (See. sec. I.6)

I. SALIENT ACCOMPLISHMENTS

This, the final, Scientific Report on AFOSR grant number AFOSR-90-0184 describes the salient accomplishments during the grant period, Feb. 01, 1990 through Mar. 31, 1993. Thirty seven publications benefitting wholly or partially (but significantly) from this support have resulted from the work done during this period. The work itself covered six major though inter-related categories. As such, the highlights noted here are divided into these six categories as outlined in the table of contents. In each of the six subsections the publications resulting from the work are noted by reference to the publication number chronologically organized in section II under List of Publications.

I. 1. GROWTH OF GaAs(111)B/$Al_xGa_{1-x}As$

: GaAs(111)B Homoepitaxy

An outstanding unsolved difficulty with the growth of GaAs on GaAs(111)B substrates had been the occurrence of pyramid-like surface structures and/or twins. We undertook to examine this phenomenon with a view to finding appropriate growth conditions under which twin-free and mirror-like surface may be simultaneously and reproducibly realized. This is the first critical step towards the growth of GaAs(111)B based heterostructures involving $Al_xGa_{1-x}As$ (i.e. unstrained) or $In_xGa_{1-x}As$ (i.e. strained) layers in which, it is believed, the existence of the piezoelectric effect may be fruitfully exploited for light modulators based on the quantum confined Stark effect (QCSE), apart from the predicted existence of non-linear optical effects.

Following our approach of systematic reflection high-energy electron diffraction (RHEED) studies to examine the correlation between growth conditions, growth kinetics, and the resulting nature of the thin films established over the past several years for GaAs(100), similar studies were carried out for the

GaAs(111)B surfaces. Having first mapped the GaAs(111)B surface reconstructions and surface "phase diagram" using the RHEED specular beam intensity from static (i.e. non-growing) surfaces, the dynamics of the specular beam was examined under various growth conditions for growths initiated in different regimes of the static surface behavior. The grown films were examined using Nomarski micrographs, scanning electron microscopy, and transmission electron microscopy. The morphological and structural behavior thus found was correlated with the RHEED behavior. Fig. 1 shows the static surface specular beam intensity as a function of the substrate temperature (T_S) at a given As_4 pressure (P_{As4}). The regimes of the surface reconstructions are also identified. It is found that twin-free epilayers with mirror-like surface morphology are reproducibly realized only for growth initiated in the region indicated by the box on the intensity plateau of the $\sqrt{19}$ x $\sqrt{19}$ reconstruction. Fig.2 shows a comparison of a GaAs film grown in this narrow window of optimized growth condition and another grown outside this window. Note the absence of twins and the mirror-like surface of the film grown in the optimized regime. Details may be found in **publications 12, 16, 21, 22 and 24**.

We note that we have, using TEM, examined the nature of the twin defects in the films grown in the non-optimized growth regime, identified these to be a rather interesting double-twin complex, and provided a possible underlying atomistic model of Ga and As incorporation during growth which may underlie the occurrence of such defects. Details are provided in **publication 16**. An atomistic model which involves surface kinetics is being examined as a reasonable starting point to examine the atomistic origins of the pyramid-like structures.

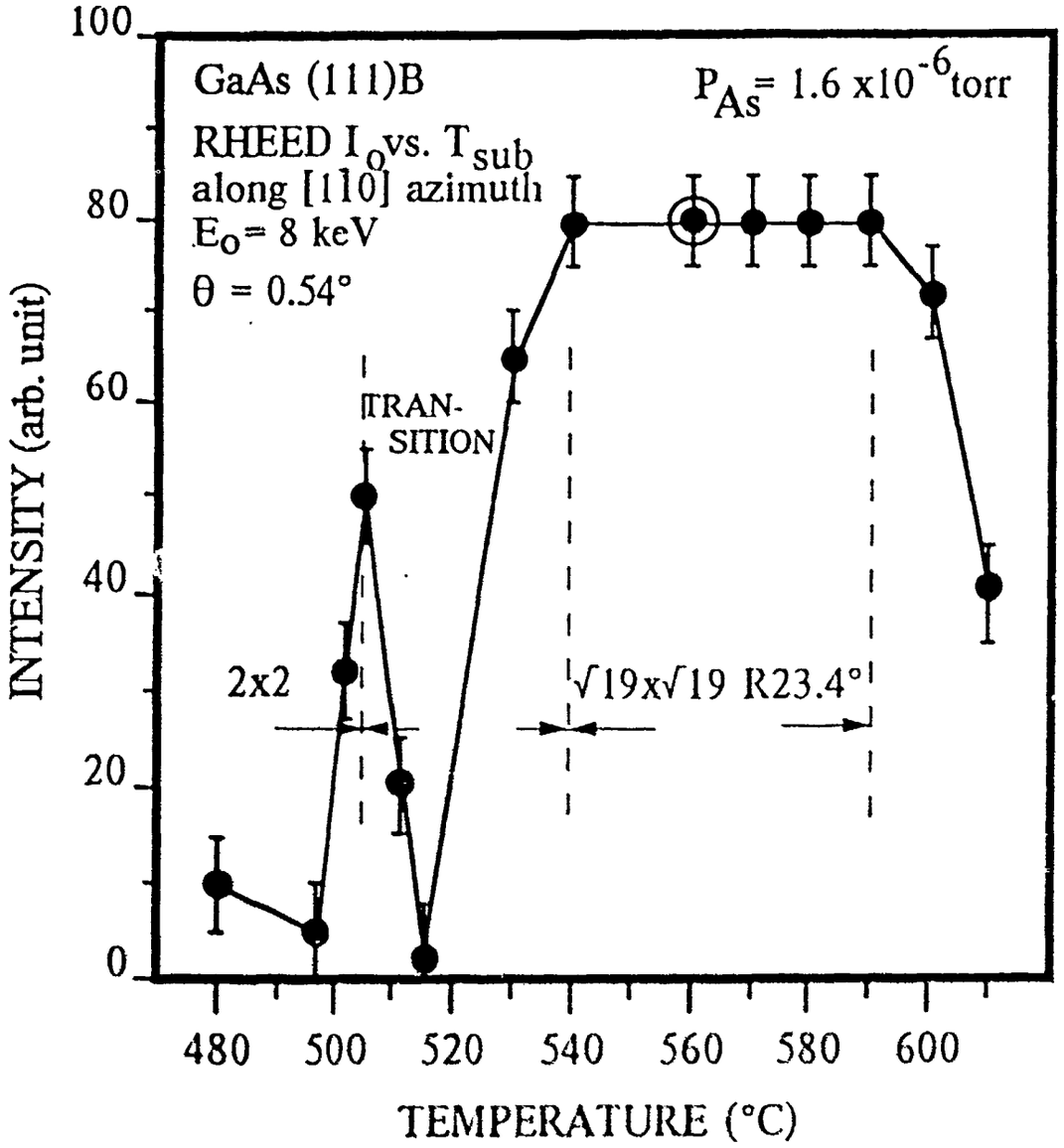
GaAs (111)B
P_{As}= 1.6 x10^{-6}torr
RHEED $I_o$vs. T_{sub}
along [1$\bar{1}$0] azimuth
E_o= 8 keV
θ = 0.54°
TRAN-
SITION
2x2
√19x√19 R23.4°
INTENSITY (arb. unit)
100
80
60
40
20
0
480
500
520
540
560
580
600
TEMPERATURE (°C)

Fig. 1

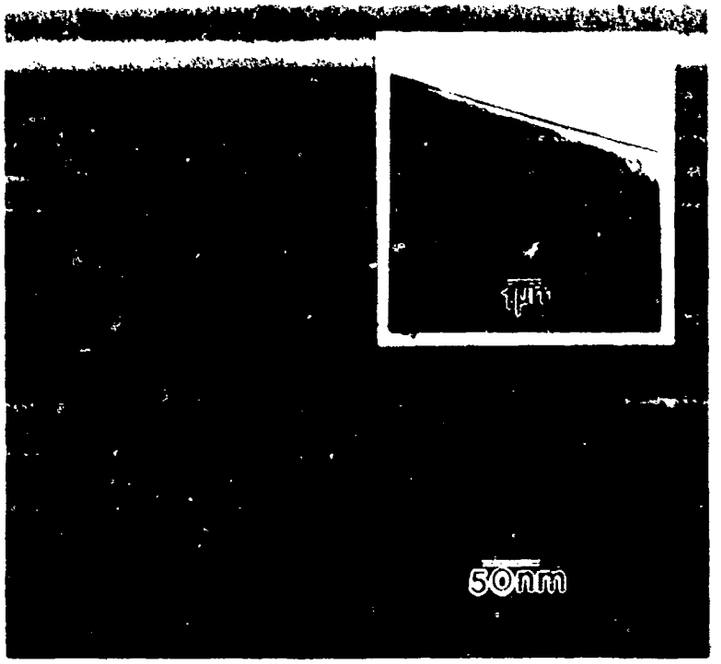
1μm
50nm

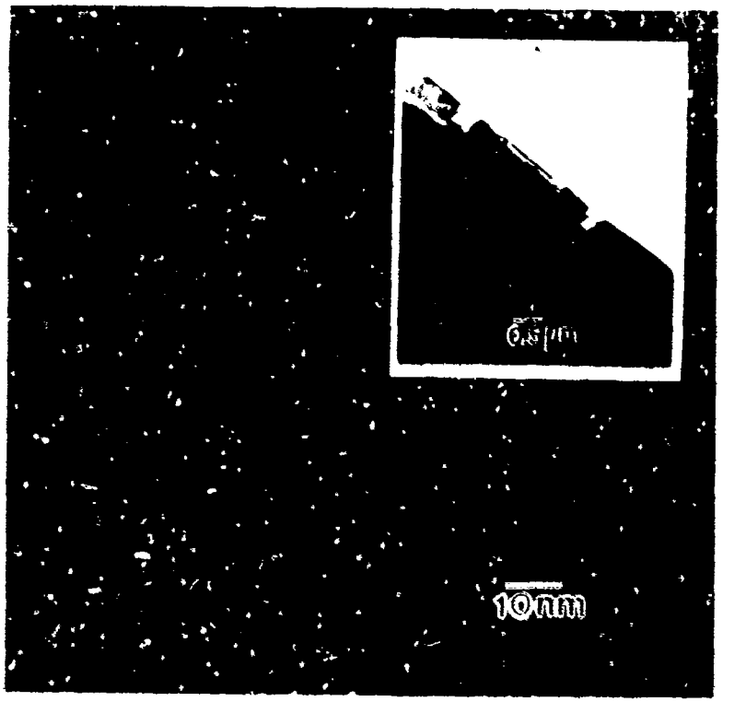
0.5μm
10nm

: GaAs(111)B/$Al_xGa_{1-x}As$ Heteroepitaxy

Following the success in achieving defect-free and specular GaAs(111)B homoepitaxy, work focussed on examining GaAs/AlGaAs heteroepitaxy on GaAs(111)B with the aim of identifying optimized and reproducible growth conditions. Note that while heteroepitaxy on misoriented GaAs(111)B is rather easily accomplished, the same had not been true for the singular surface. Studies on the RHEED behavior were carried out to identify optimized growth. High quality single and multiple GaAs/AlGaAs quantum wells were thus realized.

Next, we exploited the three-fold symmetry of the (111) surface to obtain, via photolithography followed by wet chemical etching, pyramidal mesas with triangular (111)B tops bounded by three {100} type side walls for both starting GaAs(111)B substrates and GaAs/AlGaAs MQWs grown on planar GaAs(111)B substrates. Post growth etching of the MQWs grown on planar GaAs(111)B substrates was shown to give rise to 3-dimensionally confined structures with linear dimensions as small as 150 Å. While such quantum box structures, containing as few as 22,000 atoms, are structurally the smallest volumes ever realized, the surface damage and contamination caused by post-growth processing did not permit luminescence to be observed in these structures. These results were reported in **publication 34**.

I.2. GROWTH OF STRAINED GaAs(100)/$In_xGa_{1-x}As$ STRUCTURES

: Initial stages of Growth: 3D Island and Defect Formation

Initial stages of defect formation and strain relaxation in strained heteroepitaxy has been a subject of much interest for some time the technologically important combinations Si/GaAs, Si/Si_xGe_{1-x} and $GaAs/In_xGa_{1-x}As$ receiving particular attention in recent years. Following our earlier work on

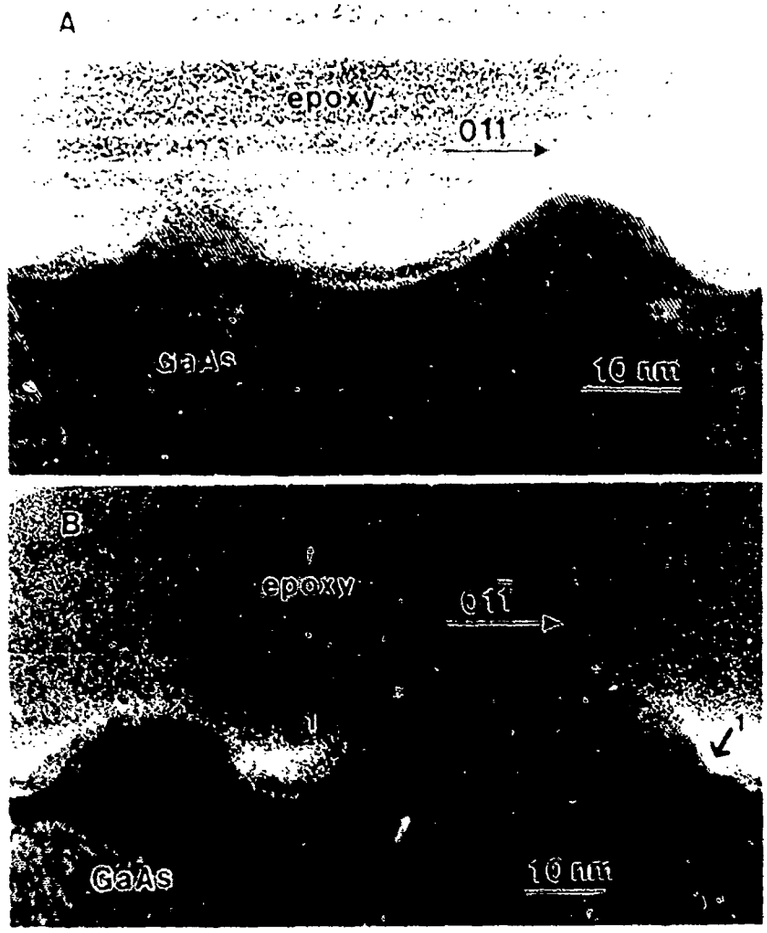

Fig. 3 : Shows coherent and incoherent islands of $In_{0.5}Ga_{0.5}As$ on GaAs (1 0 0) in the 3 D island growth mode

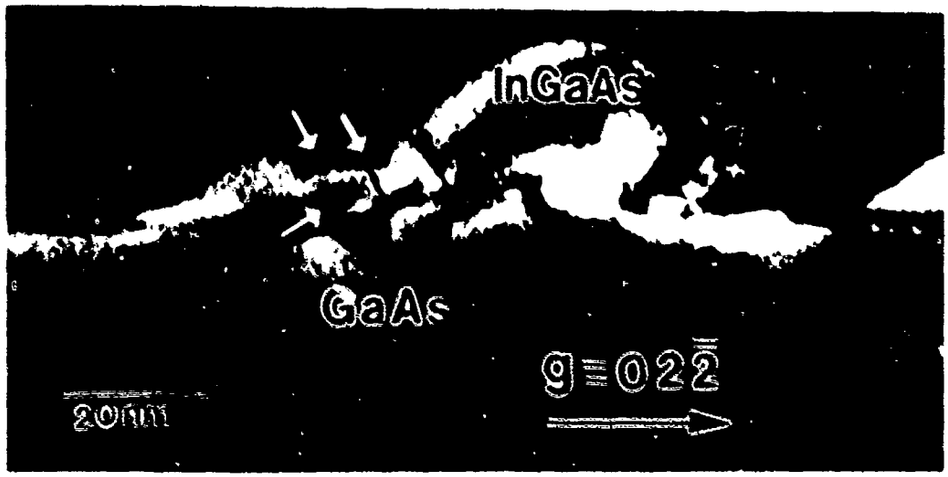

Fig. 4 : A picture showing the formation of dislocations at the interface and the grain boundaries.

the GaAs/InGaAs system, under the present grant we undertook examination of the role of the layer-by-layer and 3D island modes of growth in the onset of incoherency, i.e. defect formation, at the earliest stages of growth. Since at the high lattice mismatch (≥ 2%) occurring for In content ≥35% the strain induces 3D island formation at a growth condition dependent thickness (~8ML $In_{0.35}Ga_{0.65}As$) deposition being the maximum for the usual As-stabilized MBE, we paid particular attention to (i) the nature of defects and their formation in the 3D island growth mode regime, and (ii) the formation kinetics of the 3D islands themselves. Fig. 3 shows a cross-sectional TEM lattice image of 3D islands in a $In_{0.5}Ga_{0.5}As$ film of equivalent thickness of 7 ML deposited at 520°C. Note that small islands (typically < 200A lateral dimensions) are coherent whereas larger islands have lost coherency through the introduction of defects, nearly symmetrically, at the island edges. Although the ambiguities arising from the projection image in cross-sectional TEM prevent unambiguous conclusion, in a number of cases the location of the defect in relation to the overall island shape is highly suggestive of the possibility that defects are also introduced at the coalescence boundaries of islands. Fig. 4 shows a TEM micrograph of islands suggestive of this mechanism.

Two rather important and **new features** uncovered in these studies are, (i) the existence of **strain relaxation even in coherent islands**, and (ii) the presence of **strain in the substrate** below the islands to large depths of order 150A. Fig. 5 summarizes a typical situation for the lattice relaxation (taking fully in-plane strained InAs as the reference). Note that islands do not have the tetragonal symmetry expected of continuous coherent films. Fig. 6 shows a TEM micrograph revealing, through strain contrast, the presence of strain in the GaAs(100) substrate. These findings called into question long held (though unsubstantiated) views and historical theories relating to strained epitaxy and

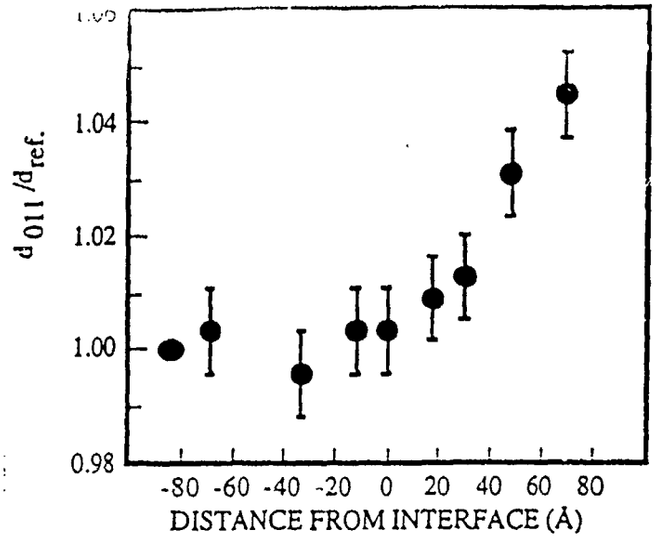

Fig. 5 : Plot of measured $(0\bar{1}1)$ interplanar spacing versus distance from the interface for a coherent island. The interplanar spacing is normalized to the lattice parameter value measured 84 A below the interface in the substrate (d_{ref})

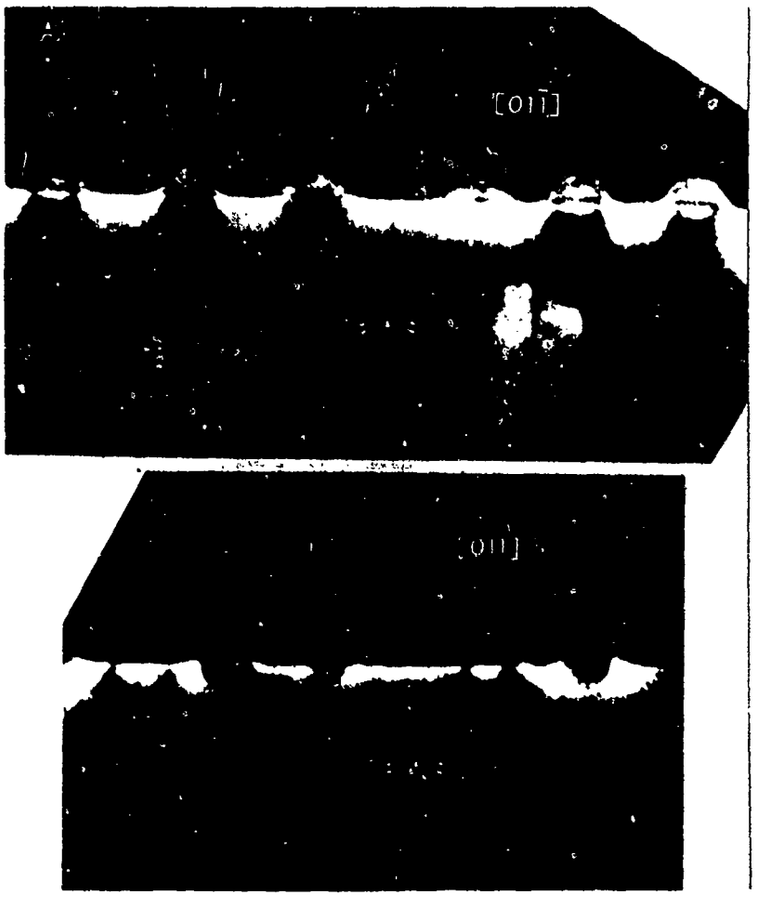

Fig. 6 : Shows existence of strain in the GaAs substrate.

have spawned a flurry of new views. Details of these results and their implications are given in **publications 10, 17 and 23.**

: 3D Island Distribution and Quantum Dots

On the subject of **the kinetics of 3D island formation** in a growth regime where such islands are purposely induced from the earliest stages of growth we initiated a systematic study as a function of (a) the growth conditions (i.e. substrate temperature, As_4 pressure, and deposition rate), (b) the deposition thickness, and (c) the deposition procedure (i.e. usual MBE, alternate deposition, As_4 controlled growth, etc.). The objective here is two-fold; (i) to examine the relative significance of the surface kinetic processes such as group III migration, group V incorporation, the role of incorporation at island edges and the possible connection with strain relaxation without or with defect formation, and (ii) the possibility of realizing 3-dimensionally confined nanostructures (i.e. so-called quantum dots) in the form of coherently strained and fairly uniform sized 3D islands of InGaAs, eventually placed in a regular array via growth on pre-patterned mesas (see sec. I.5). The results noted above and illustrated via figs. 3 through 6 point to such a possibility. The role of strain relief in the substrate under and near the islands as discovered in the above noted results is of particular significance to these objectives.

For the studies of 3D island formation and identifying optimal conditions for obtaining a range of coherent island average sizes with very narrow distribution we chose to focus on the binary InAs islands rather than the alloys. This choice was motivated by the recognition that while our results on $In_{0.5}Ga_{0.5}As$ islands (figs. **5** and **6**) were instrumental in uncovering new effects, the interpretation of the lattice relaxation in the islands is complicated by the uncertainty of In content variation from island to island and In segration towards

the surface in the islands themselves. Earlier computer simulation work on InGaAs island formation carried out in our group indicates that the strain producing species (e.g. In in GaAs) has a preferred migration rate for upwards inter-planar migration as this tends to lower the island energy due to greater strain relaxation. The possible In content variation in alloy islands has thus prevented a reliable theoretical analysis of the strain relaxation data of fig. 5. Indeed, attempts to fit expressions derived on the basis of the tradtional thermodynamic arguments based on the energetics alone reveal serious discrepancies as discussed in the Ph.D. dissertation of S. Guha (University of Southern California, 1991).

Samples of InAs islands formed on GaAs(100)±0.1° substrates were grown as a function of T_S (the substrate temperature) at a fixed P_{As4} (arsenic pressure), τ_{In} (the In monolayer delivery time), and total amount (d) of InAs deposited (from 4ML to 8ML). Likewise, samples were grown as a function of another parameter, keeping the others fixed (e.g. P_{As4} while T_S, τ_{In}, and d are kept fixed). While at the end of the present grant period examination of such samples was continuing, the first results on the island density, average island size, and the lateral size limit for transition from coherent to incoherent islands have already revealed some important results that are at odds with conventionally held beliefs and models. Figs. 7 through 9 summarize the early findings. Shown is the dependence of the island density determined from plan view TEM on the substrate temperature (fig. 7a) and As_4 pressure (fig. 7b). The former behavior of increasing island density with decreasing T_S is experimentally observed to be accompanied with a decrease in the average lateral size of the island. (The islands are observed to have their base edges oriented along <010> and <001> directions, are essentially square in shape, and have {10h} type side

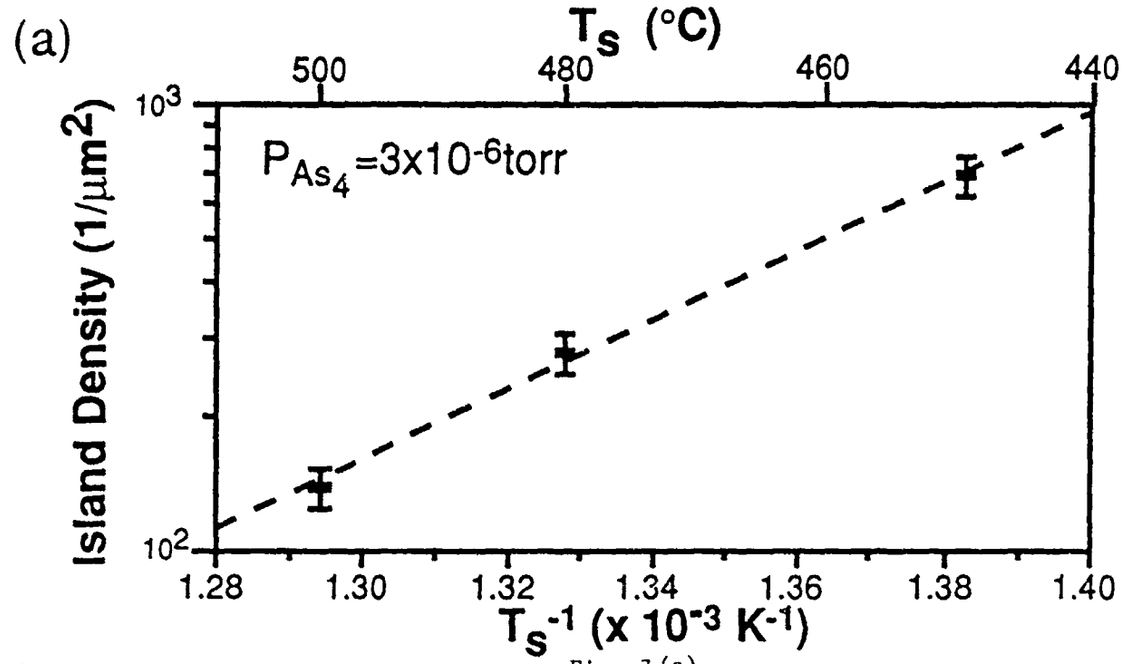
(a)
T_S (°C)
500
480
460
440
10^3
10^2
P_{As_4}=3x10^{-6}torr
Island Density (1/μm^2)
1.28
1.30
1.32
1.34
1.36
1.38
1.40
T_S^{-1} (x 10^{-3} K^{-1})

Fig. 7(a)

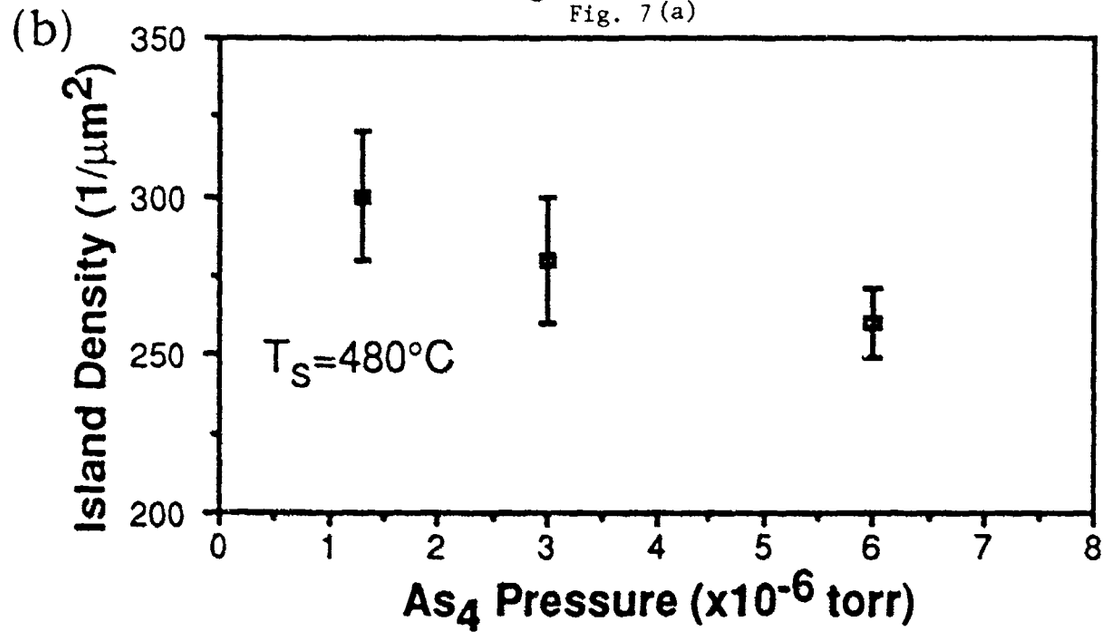
(b)
350
300
250
200
Island Density (1/μm^2)
T_S=480°C
0
1
2
3
4
5
6
7
8
As_4 Pressure (x10^{-6} torr)

Fig.7(b)

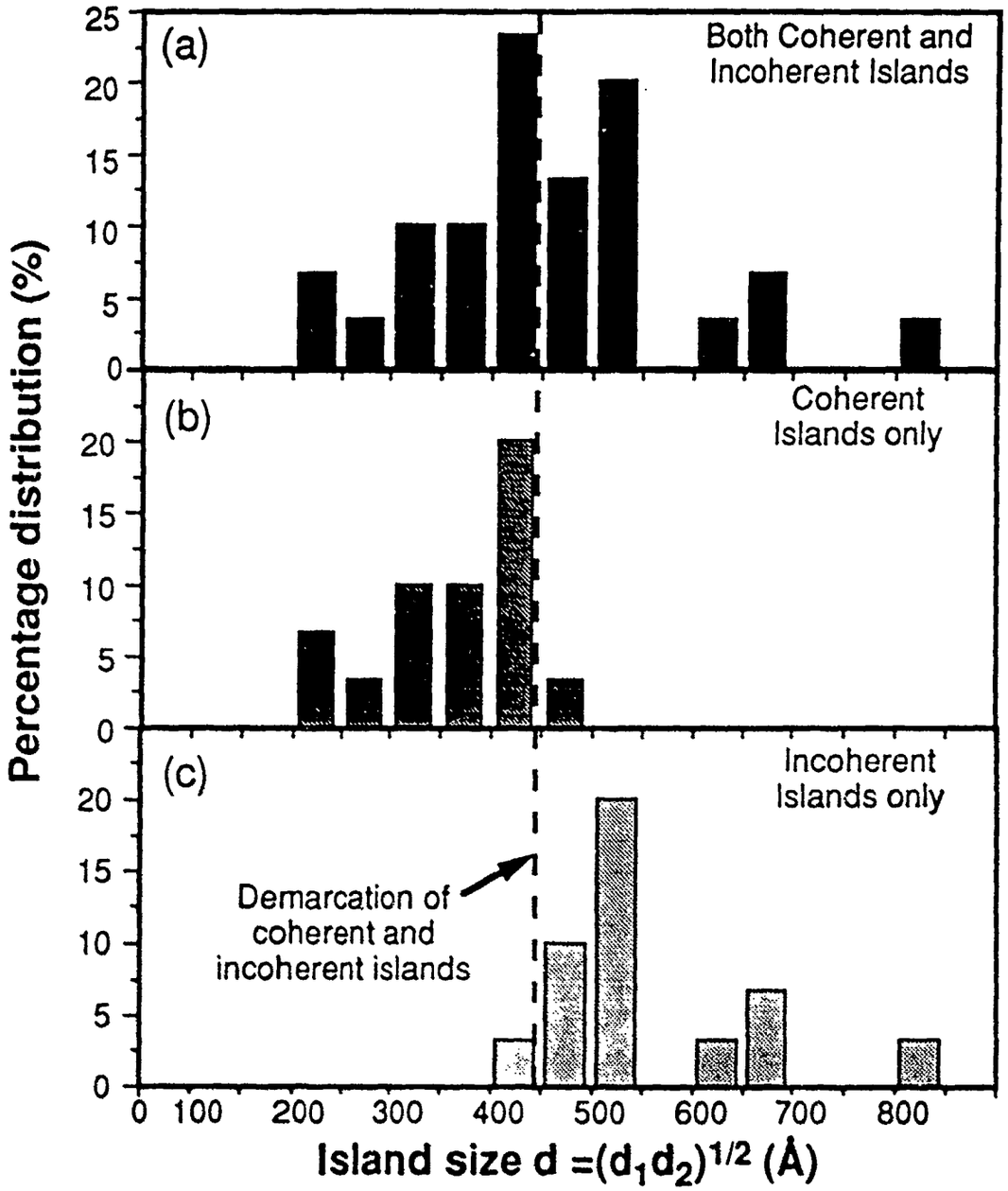
(a)
Both Coherent and Incoherent Islands
(b)
Coherent Islands only
(c)
Incoherent Islands only
Demarcation of coherent and incoherent islands
Percentage distribution (%)
Island size d =(d1d2)1/2 (Å)
0
5
10
15
20
25
0 100 200 300 400 500 600 700 800

Fig. 8

facets). By contrast, the island density is seen to decrease with increasing P_{As4} but the average lateral size of the islands is observed to remain essentially constant within the statistical accuracy. While within conventional framework one may be tempted to reconcile the T_S dependence as being due to enhanced In migration with increasing T_S, that this is not the complete story of the kinetics of 3D island formation is evident from the behavior with respect to increasing P_{As4} since the latter, within the same conventional framework, would imply a decrease in the In migration and hence an increase in island density if the island formation were being predominantly controlled by In surface diffusion. At this point we are of the view that the atom (In and As_4) incorporation kinetics at the island edges and the kinetics of new island initiation, are also playing a significant competing role in the formation of 3D islands. Our previous computer simulations give credance to this view as they have shown, via comparison to the RHEED intensity dynamics, that the strain relaxation in the islands, particularly at the island edges that provide steps (albeit very short) and kink sites, affects the atom incorporation kinetics rather seriously. Yet another experimental evidence that the 3D island formation is not merely In diffusion controlled is found in the slope of the fit to the data in fig. 7a. The slope is 1.54eV/k_B which, if translated into an activation energy for In surface diffusion using conventional models of diffusion controlled island formation, would give an activation evergy ranging from 4.5eV to 5.4eV, entirely too high and unphysical a range.

Figure fig. 8(a) shows the distribution of island sizes in a sample grown at 480°C at $P_{As4} = 3 \times 10^{-6}$ Torr, τ_{In} = 8 sec and for a total depostion of 6MLs. Panels (b) and (c) show the distribution of only coherent and incoherent islands, respectively, the demarcation being a ~400°A. The coherent/incoherent nature was determined by exploiting the continuity or lack thereof of the Moire fringes in

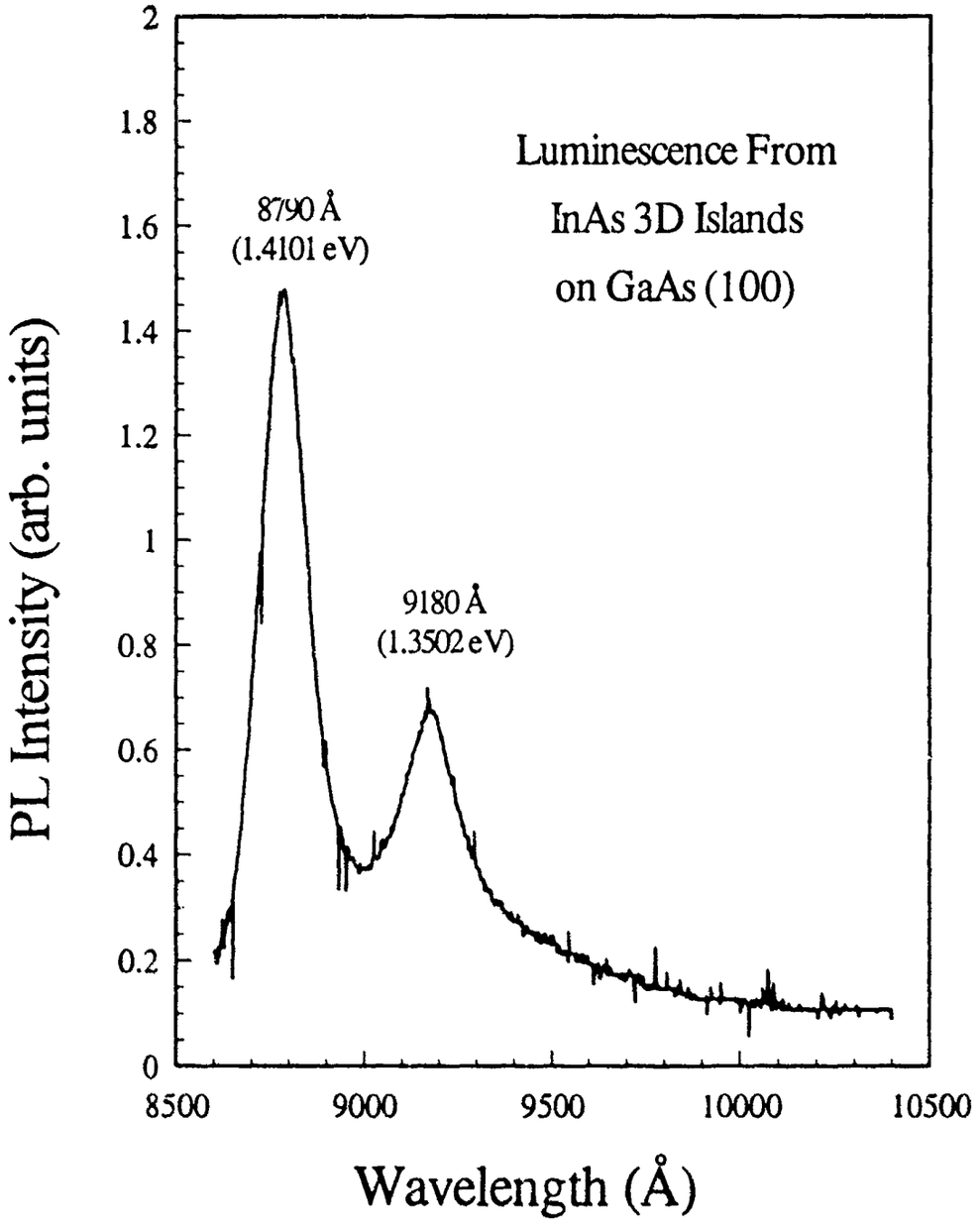
Luminescence From
InAs 3D Islands
on GaAs (100)
8790 Å
(1.4101 eV)
9180 Å
(1.3502 eV)
PL Intensity (arb. units)
Wavelength (Å)
0
0.2
0.4
0.6
0.8
1
1.2
1.4
1.6
1.8
2
8500
9000
9500
10000
10500

Fig. 9

the islands and the correspondence checked independently against high resolution lattice imaging of several islands. Figure 9 shows that even without a protective layer the 3D InAs islands luminesce at dramatically blue shifted wavelengths. This thus indicates that, on pre-formed mesas of linear dimensions ≤400°A (see sec. I.5), a deposition of InAs under these conditions can lead to a regular array of 3D islands of uniform size placed in a regular array and acting like quantum dots. Work in this direction is continuing under the new AFOSR grant.

: Strain Relief via Patterned Growth - Variations across the mesa

We have previously, under AFOSR sponsored work (AFOSR Grant No. 86-0166), demonstrated the notion that growth of strained layers on substrates containing pre-patterned mesas permits growths to thicknesses as much as seven times those at which dislocations and other extended defects get introduced for growth on non-patterned substrates. The underlying reasoning invoked to expect this was that strain relief was expected to be provided by the presence, at the mesa edges, of the free surface of the grown film. To examine this underlying idea further we undertook growths, on GaAs(100) substrates patterned with mesa stripes down to 1 μm widths, of single epilayers of $In_xGa_{1-x}As$ films with various x and of thicknesses ranging from below to above the nominal critical thickness for dislocation generation on non-patterned substrates. These films were examined via cross sectional TEM and, in collaboration with Drs. Wade Tang and Hal Rosen of IBM Almaden Research Center (San Jose, CA), via micro-Raman scattering measurements to obtain the **spatial variation in the strain across the mesa width**, the side wall growth, and the growths in the valleys between the mesas. Through measurements of the LO and TO phonon induced Raman shifts, relative intensities, the line shapes, and the

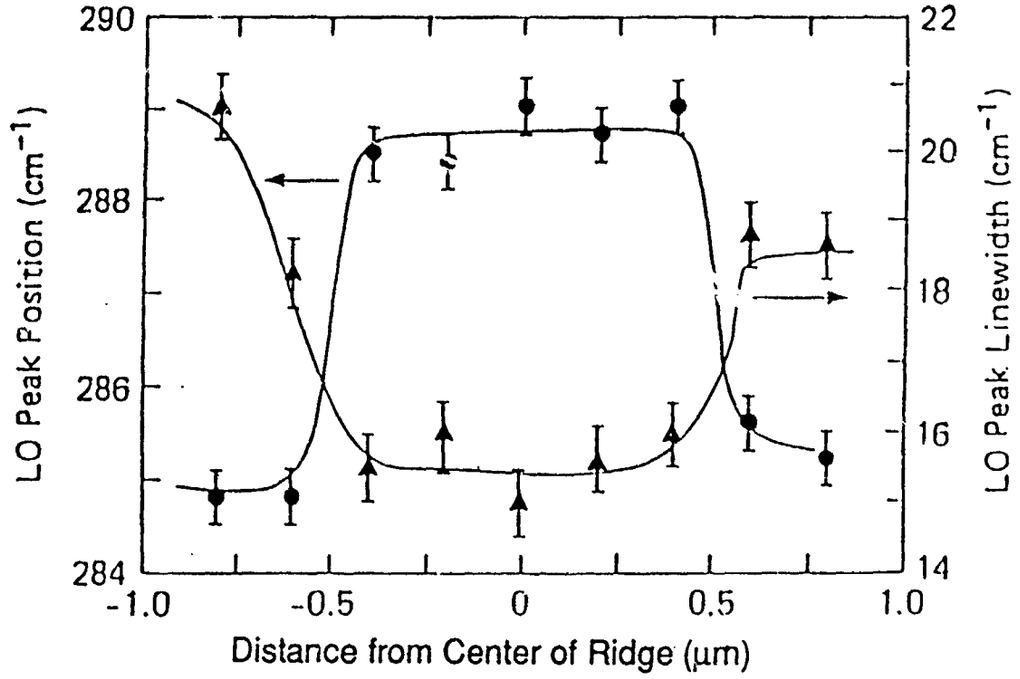
290
288
286
284
22
20
18
16
14
-1.0
-0.5
0
0.5
1.0
LO Peak Position (cm^{-1})
LO Peak Linewidth (cm^{-1})
Distance from Center of Ridge (μm)

Fig. 10

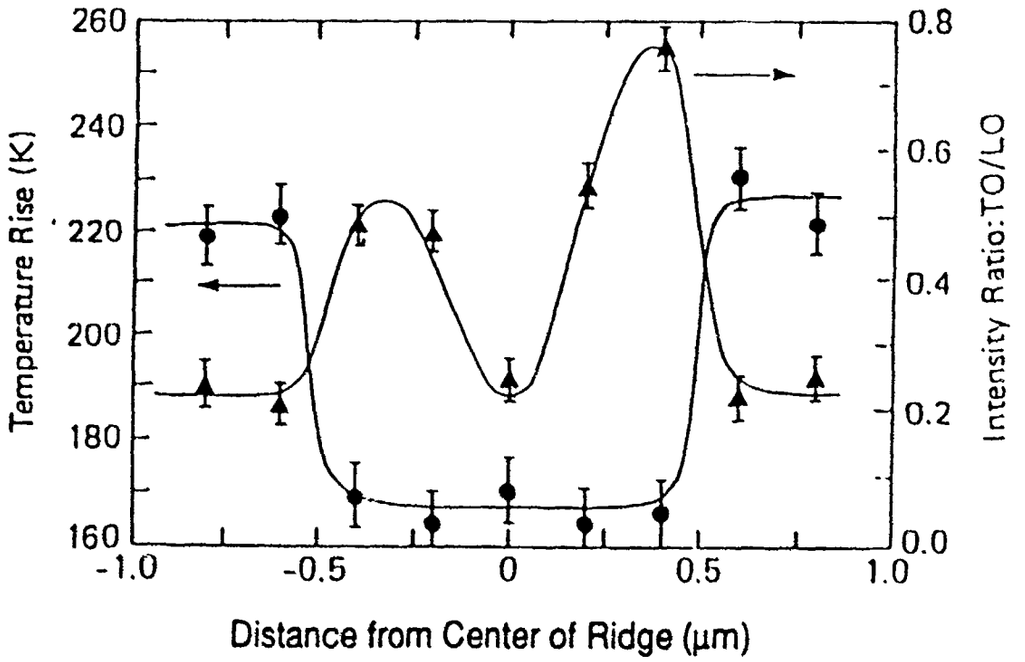
260
240
220
200
180
160
0.8
0.6
0.4
0.2
0.0
-1.0
-0.5
0
0.5
1.0
Temperature Rise (K)
Intensity Ratio:TO/LO
Distance from Center of Ridge (μm)

Fig. 11

Stokes-AntiStokes relative intensities, a measure of the spatial distribution of strain and its relation with the TEM observations of the nature of the defects and their density was obtained for the first time. This has provided evidence for the essential correctness of our ideas regarding strain relief in patterned growth. Fig. 10 shows a typical finding for the LO phonon induced Raman shift as one scans across the mesa top into the valley region. Fig. 11 shows the behavior of the temperature rise. Details of these findings may be found in **publication 20**

I.3. HIGHLY STRAINED, HIGH In & Al CONTENT GaAs(100)/$In_xGa_{1-x}As/Al_yGa_{1-y}As$ SINGLE AND MULTIPLE QUANTUM WELLS

While the growth of strained GaAs/$In_xGa_{1-x}As$ single epilayers described in the preceding section allowed examination of the kinetics of the initial stages of growth and of a means of defect reduction, the understanding so gained was exploited under the present grant to address fundamental issues relating to growth of high quality highly strained $Al_yGa_{1-y}As/In_xGa_{1-x}As$ single and multiple quantum well structures involving $0.2 < x < 0.35$ and $0.3 \leq y \leq 1$ (i.e. high Al content barriers) and relevant to applications in such devices as resonant tunneling diodes, pseudomorphic HEMTs and MISFETs, and optical light modulators. This class of structures present growth challenges originating in two different aspects; (i) The high In content means high strain ($\Delta a/a \sim 2\%$ at $x = 0.3$) with a concomitant tendency towards 3-D island formation (i.e. Stranski-Karastanov growth mode) and a rather low (~100 Å) theoretically predicted critical thickness for misfit dislocation formation even if a planar film morphology could be realized (This, in practice, is not the case as the Stranski-Karastanov growth mode sets in at an earlier thickness) (ii) The vastly differing congruent evaporation temperatures of AlAs, GaAs, and InAs and their alloys also present challenges of finding optimized growth conditions giving sufficient surface mobility for all group III species without losing In via evaporation.

Table 1. Structures and the corresponding Exciton transition energies & FWHM of the Single Quantum Wells.

Structure No	Growth Log #	Lower Barrier	Well	Upper Barrier	Transition Energy(eV)	FWHM (meV)
No. 1	RG9104090111	GaAs	$In_{0.26}Ga_{0.74}As$	GaAs	1.243	8.0
No. 2	RG9104130111	GaAs	$In_{0.26}Ga_{0.74}As$	$Al_{0.30}Ga_{0.70}As$	1.265	5.2
No. 3	RG9012040111	GaAs	$In_{0.26}Ga_{0.74}As$	$Al_{0.47}Ga_{0.53}As$	1.232	5.8
No. 4	RG91041302C	GaAs	$In_{0.26}Ga_{0.74}As$	$Al_{0.70}Ga_{0.30}As$	1.265	9.3
No. 5	RG90120702F	GaAs	$In_{0.26}Ga_{0.74}As$	AlAs	1.233	7.4
No. 6	RG91030202G	$Al_{0.30}Ga_{0.70}As$	$In_{0.26}Ga_{0.74}As$	$Al_{0.30}Ga_{0.70}As$	1.242	5.4
No. 7	RG910411018	$Al_{0.30}Ga_{0.70}As$	$In_{0.26}Ga_{0.74}As$	$Al_{0.47}Ga_{0.53}As$	1.258	7.3
No. 8	RG910124011F	$Al_{0.30}Ga_{0.70}As$	$In_{0.26}Ga_{0.74}As$	$Al_{0.70}Ga_{0.30}As$	1.252	11.5
No. 9	RG9104130111	$Al_{0.30}Ga_{0.70}As$	$In_{0.26}Ga_{0.74}As$	AlAs	1.255	7.4
No.10	RG91030202G	$Al_{0.47}Ga_{0.53}As$	$In_{0.26}Ga_{0.74}As$	$Al_{0.47}Ga_{0.53}As$	1.262	5.8
No.11	RG910124011F	$Al_{0.70}Ga_{0.30}As$	$In_{0.26}Ga_{0.74}As$	$Al_{0.70}Ga_{0.30}As$	1.255	5.1
No.12	RG91030501A	AlAs	$In_{0.26}Ga_{0.74}As$	AlAs	1.253	7.6
No.13	RG91081201B	$(AlAs)_3(GaAs)_7$	$In_{0.26}Ga_{0.74}As$	$(AlAs)_3(GaAs)_7$	1.290	4.3
N0.14	RG91081202C	$(AlAs)_4(GaAs)_5$	$In_{0.26}Ga_{0.74}As$	$(AlAs)_4(GaAs)_5$	1.245	7.2
No.15	RG91081203G	$(AlAs)_5(GaAs)_2$	$In_{0.26}Ga_{0.74}As$	$(AlAs)_5(GaAs)_2$	1.242	7.5

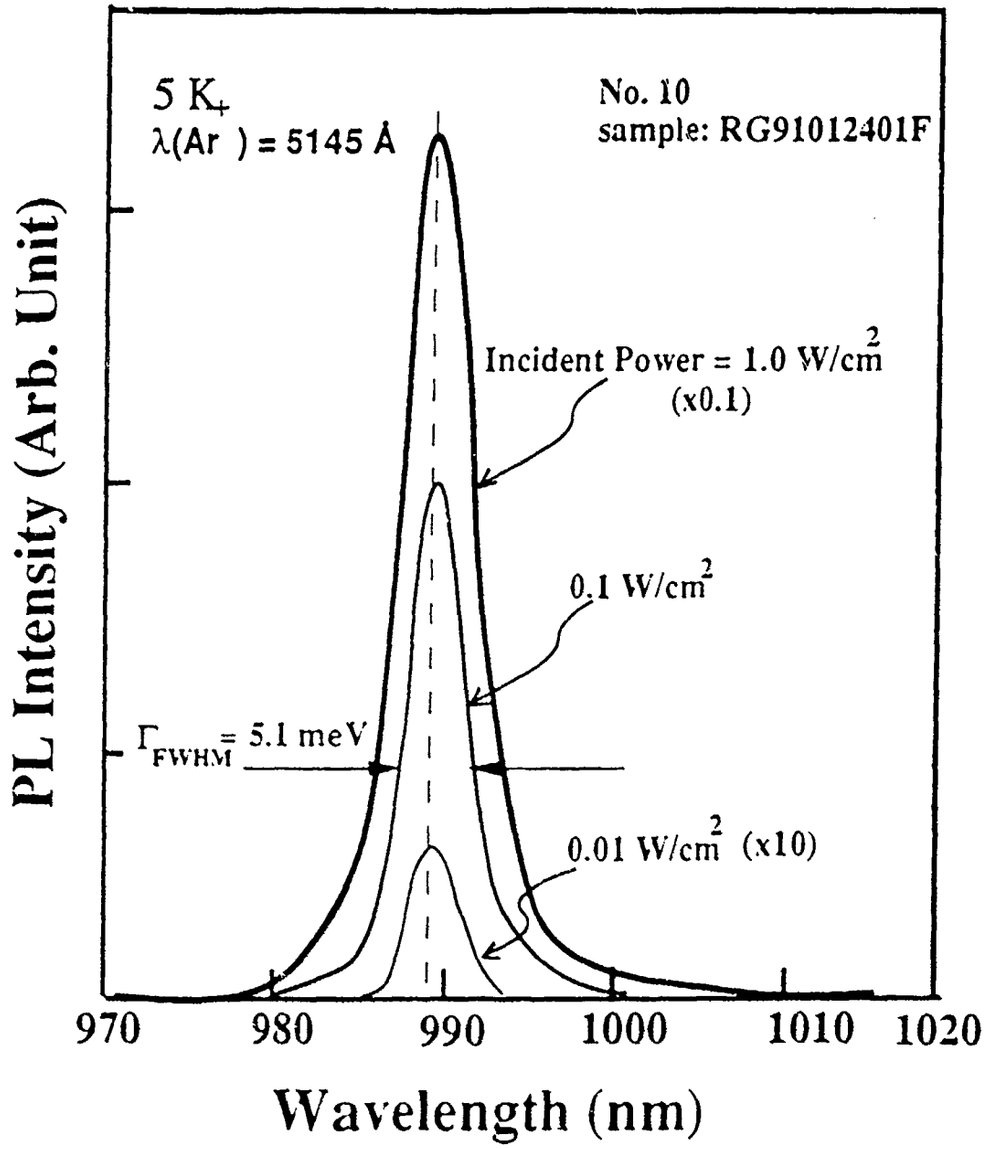

Fig. 12 PL spectra for $Al_{0.70}Ga_{0.30}As$ /$In_{0.26}Ga_{0.74}As$ / $Al_{0.70}Ga_{0.30}As$ SQW at 5 K as a function of the incident power.

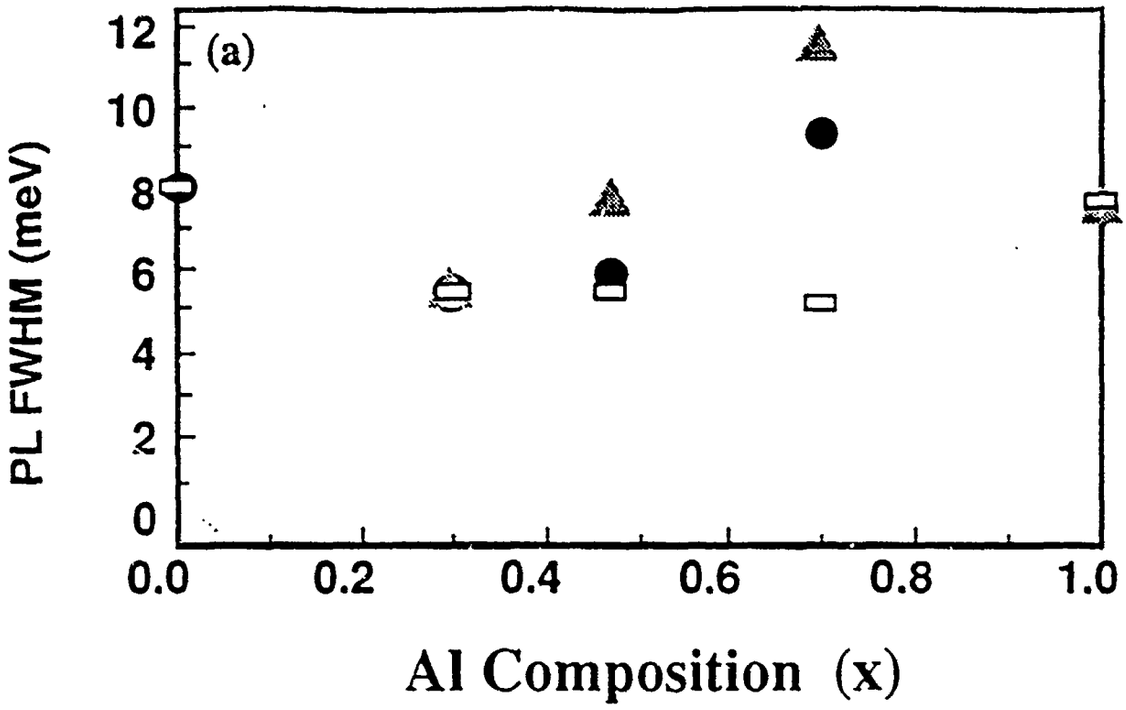
(a)
PL FWHM (meV)
12
10
8
6
4
2
0
0.0
0.2
0.4
0.6
0.8
1.0
Al Composition (x)

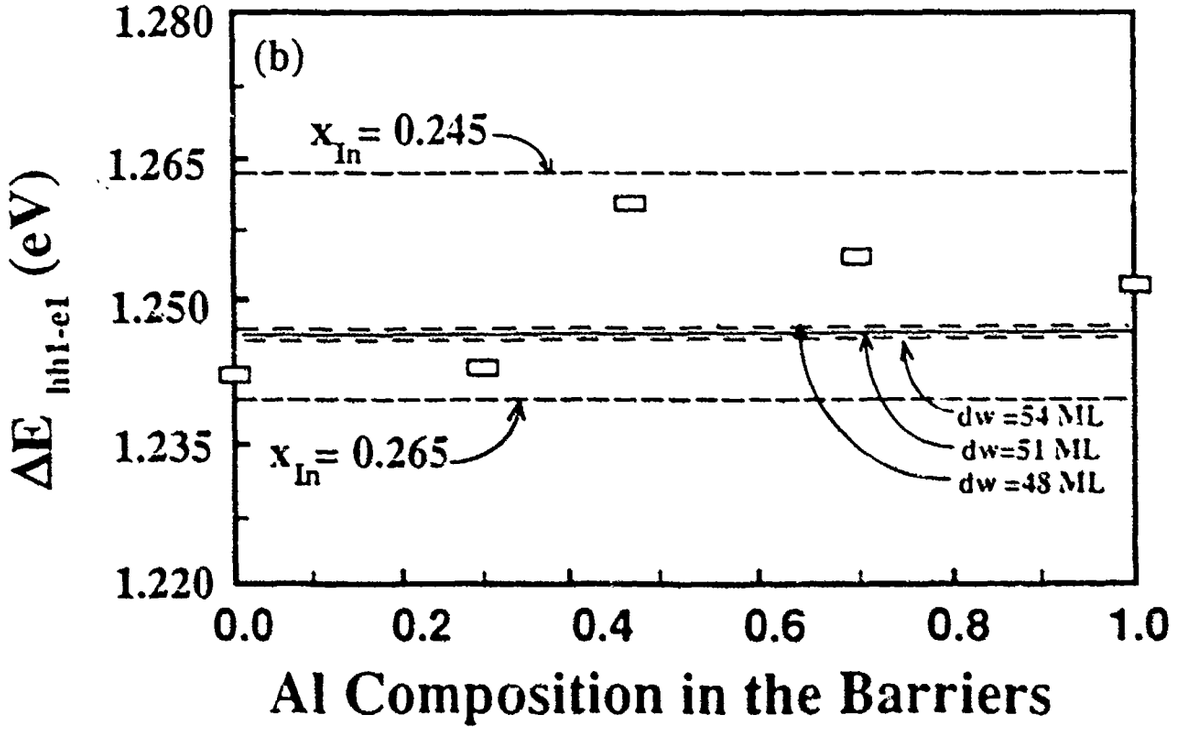
(b)
$\Delta E_{hh1\text{-}e1}$ (eV)
1.280
1.265
1.250
1.235
1.220
x_{In} = 0.245
x_{In} = 0.265
dw =54 ML
dw=51 ML
dw =48 ML
0.0
0.2
0.4
0.6
0.8
1.0
Al Composition in the Barriers

Fig. 13

: Single Quantum Wells

Once again, using RHEED behavior and growth interruption, we identified appropriate regime of growth conditions for such simultaneously high In and Al bearing structures. A large number of $Al_yGa_{1-y}As/In_xGa_{1-x}As/Al_zGa_{1-z}As$ single quantum well structures with y=z (i.e. symmetric) or y≠z (i.e. asymmetric) confining potential profiles were grown systematically as a function of y and z for different values of x (but mostly x = 0.26 and 0.3) and well widths. These structures were examined via photoluminescence (including temperature and power dependent studies) and supplemented, where thought appropriate, by high resolution transmission electron microscope studies (the latter were carried out under other support). High PL efficiencies accompanied by the narrowest linewidths (5 meV to 6 meV) ever reported in such structures were achieved. The behavior of an illustrative set of samples is shown in Table 1. Fig. 12 shows the PL behavior for y = z = 0.7 and x = 0.26. To systematically analyze the PL behavior as a function of the structural and chemical parameters, theoretical modelling including strain effects was carried out and the results compared to the experimental findings. The comparison revealed that the dominant cause of the observed fluctuations in the PL peak position (see Fig. 13) is the variation in the In content by ± 1% across the sample in a given run as well as in the same area from run-to-run. The latter is a consequence of the accuracy with which RHEED can help control the fluxes at typical growth rates of 0.5 ML/sec. These results were reported in **publications 35, 43, 44**. Further details may be found in, K. Kaviani, Ph.D. Dissertation, (University of Southern California, 1993).

: Resonant Tunnelling Diodes

Following through on our earlier success in realizing strained $In_xGa_{1-x}As/AlAs$, $x \leq 0.20$ resonant tunneling structures grown directly on GaAs(100),

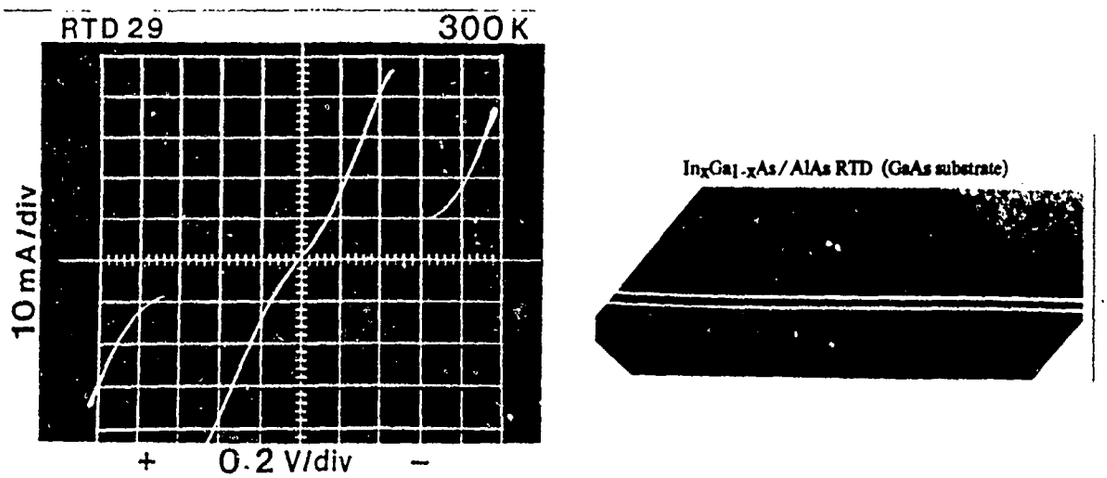

(a) (b)

Fig. 14 (a) DC I-V characteristics from 12 μm x 12 μm mesas of RTD #29 with AlAs barriers and conventional alloy $In_{0.3}Ga_{0.7}As$ spacer andwell regions. This device shows a J_p of 32 kA/cm^2 with a PVR of 5.2 at 300 K.

(b) TEM micrograph of RTD #28 showing highly abrupt and smooth interfaces.

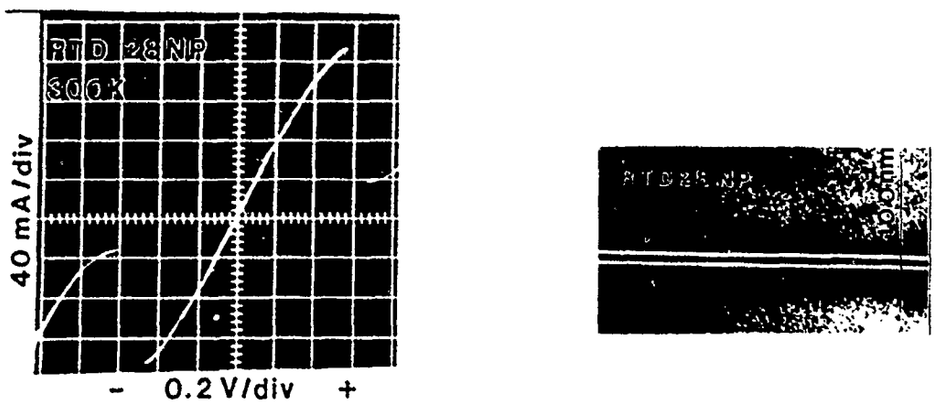

(a) (b)

Fig. 15 (a) DC I-V characteristics from 12 μm x 12 μm mesas of RTD #28 with AlAs barriers, short period multiple quantum well (SPMQW) type $In_{0.33}Ga_{0.67}As$ well and SPMQW type $In_{0.2}Ga_{0.8}As$ spacer regions. This device shows a J_p of 125 kA/cm^2 with a PVR of 4.7 at 300 K. (b) TEM micrograph of RTD #28 showing highly abrupt and smooth interfaces.

under the present grant we pursued growth of RTD's with x> 0.25. This regime is particularly challenging from the MBE growth view point since, depending upon the growth conditions, a change from the layer-by-layer (i.e. 2D) growth mode to 3D island growth mode occurs at needed film thicknesses for x between 0.25 to 0.30. Employing $In_{0.33}Ga_{0.67}As$ alloys as the spacer and well regions and AlAs as the barrier regions, and using RHEED determined growth conditions, we were able to control the growth (i.e. suppress 3D islanding) sufficiently well to obtain the results shown in fig. 14. Beyond 33% In suppressing the 3D island formation tendency sufficiently to achieve the degree of interface perfection required by a quantum interference effect based device such as an RTD was not successful for the InGaAs film thicknesses desired for appropriate design of the RTDs. Consequently we turned to exploiting short period multiple quantum wells (SPMQW) of InAs/GaAs as the spacer and well regions, the barrier regions still being AlAs. In fig. 15 are shown the dc I-V characteristics as well as the cross section electron microscope image contrast of a sample containing $(InAs)_1/(GaAs)_4$ and $(InAs)_1/(GaAs)_2$ SPMQW as the former and well regions, respectively. The former thus corresponds to an "equivalent" alloy concentration of 20% and the well to 33%. One notes a significant improvement in the room temperature peak current density (125 KA/Cm^2 compared to 32 KA/Cm^2 in fig. 14) without any significant loss in the peak-to-valley ratio. Details of these results may be found in **publication 25**. Further details, including theoretical analysis of the RTD I-V characteristics, may be found in **publications 11 and 18** and in, R.M. Kapre, Ph.D. Dissertation, University of Southern California, 1991.

It may be worth noting that the simultaneously high room temperature peak current density (>100KA/Cm^2) and peak-to-valley ratios ($\geq$5) achieved in 1990 not only remain amongst the best achieved to-date in the strained InGaAs/AlAs system grown directly on the GaAs substrate but are in a regime of

practical value. This, combined with the transparent nature of the GaAs substrate for the operating wavelength regime of InGaAs/InAlGaAs based optical devices, opens the way for monolithic integration of such RTD's with modulator and detector devices, such as proposed for the monolithic opto-electronic transistor (MOET). The results obtained here were therefore used as a leverage for demonstrating the first realization of the MOET within all III-V electronic (RTD and MESFET) and optoelectronic (detector and modulator) components as a potential candidate for a digital optical switch in the context of the AFOSR sponsored USC URI on Integration of Optical Computing in which this principal investigator has been a participant.

: Multiple Quantum Wells and Electro-absorption

The quantum confined Stark-effect based electroabsorption and electrorefraction behavior of MQWs offers much potential for realizing appropriate light modulators for digital and analog applications. The strained GaAs/InGaAs based MQW's offer an operating wavelength regime for which the GaAs substrate is transparent, thereby eliminating the necessity of patterned etching of the substrate faced in the GaAs/AlGaAs system when working in the transmission geometry. In the reflection geometry, the transparency of the substrate allows for through-substrate reflection modulators which opens the possibility of a face-to-face bonding between the III-V MQW modulator bearing chip and Si-based detection and addressing circuitry on a Si chip. Motivated by such considerations, under the present grant we examined the RHEED based growth conditions for the realization of high quality GaAs/$In_xGa_{1-x}As$ ($x \leq 0.20$) MQW's of total thickness between 1 μm and 1.5 μm grown on n^+ - GaAs(100) non-patterned substrates and capped with a p^+ GaAs capping layer. The p-

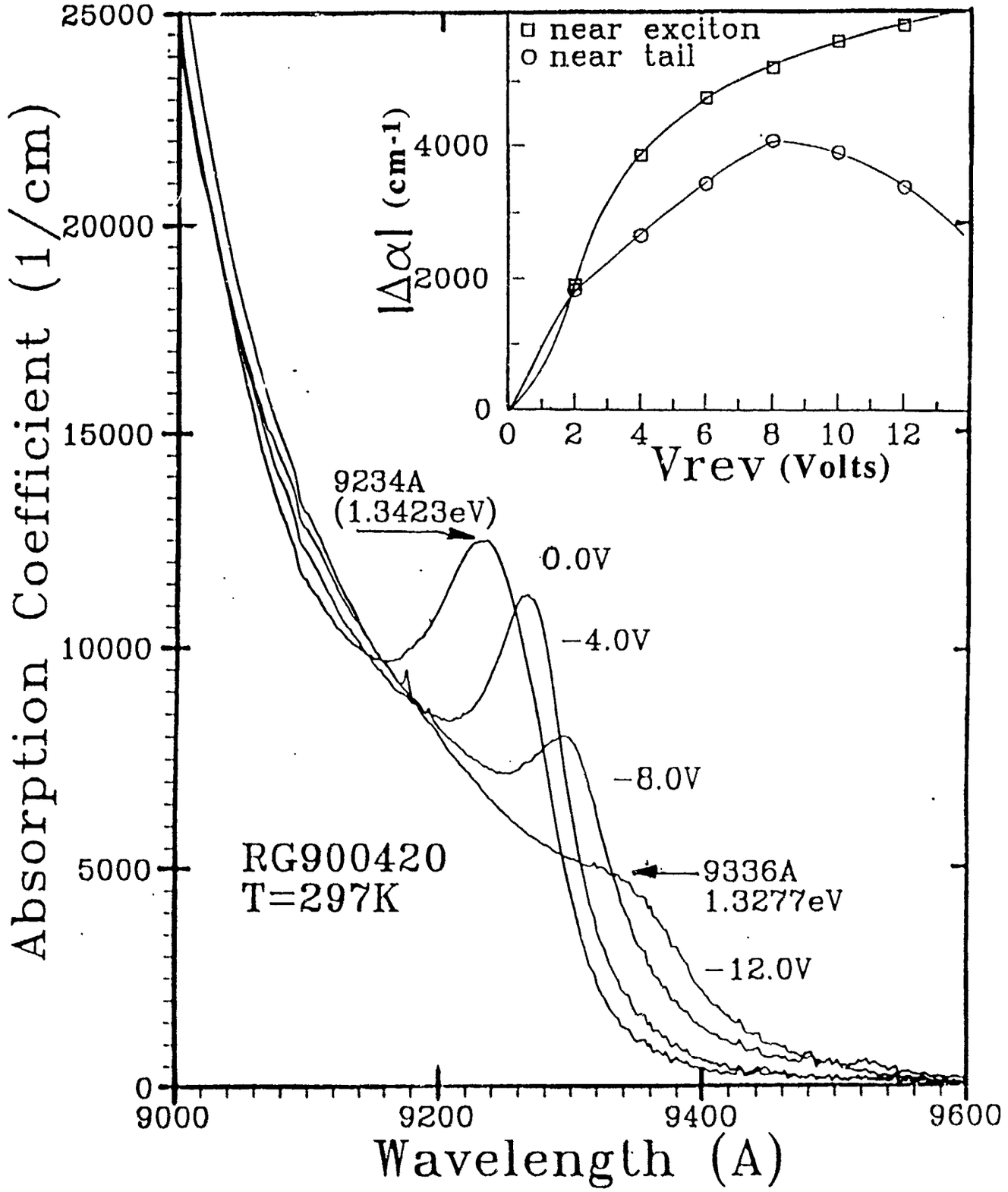
Absorption Coefficient (1/cm)
25000
20000
15000
10000
5000
0
9000
9200
9400
9600
Wavelength (A)
9234A
(1.3423eV)
0.0V
-4.0V
-8.0V
9336A
1.3277eV
-12.0V
RG900420
T=297K
□ near exciton
○ near tail
|Δα| (cm-1)
4000
2000
0
0 2 4 6 8 10 12
Vrev (Volts)

Fig. 16

i(MQW)-n configuration thus permits application of reverse bias and therefore examination of the absorption behavior under applied electric fields as well.

An illustrative example of the room temperature electroabsorption behavior for a 50 period GaAs(70 ML)/$In_{0.13}Ga_{0.67}As$(35 ML) MQW (total thickness 1.486 μm) is shown in fig. 16. Apart from the high quality of the MQW manifest in a remarkably narrow exciton linewidth for such a thick MQW, a feature observed for the first time is the **initial narrowing** of the exciton line up to -4V bias, before broadening sets in due to the well-known tunnelling effect. This revealed, for the first time, that at zero bias the built-in field is highly inhomogeneously distributed through the "intrinsic" MQW region in the p-i(MQW)-n structure - a feature long suspected but never before seen in optical behavior. We thus demonstrated that the zero-bias linewidth in MQW's is not necessarily a true reflection of the intrinsic quality of the sharpness of individual wells but rather manifests the convolution of slightly shifting excitonic transition energy from well to well due to the spatially varying built-in field arising from the background doping. This was confirmed via independent C-V measurements on similar samples which showed that a reverse bias between 4V and 5V was needed to deplete the intrinsic region. The 5.5 meV room temperature linewidth at -4V in fig. 16 narrows to a remarkable 2.5 meV at 77K testifying to the degree of growth control afforded by a systematic and judicious use of RHEED in obtaining kinetically optimized growth conditions.

The inset in fig. 16 shows the maximum change in the absorption coefficient ($\Delta\alpha$) near the zero bias exciton peak and in the tail region as a function of the applied reverse bias. Finally, in fig. 17 we have summarized the behavior of $\Delta\alpha$ as a function of applied electric field (to achieve normalization with respect to the MQW thickness and accounting for the built-in electric field) for our sample and other results in the liteature. As can be seen, at low electric fields -

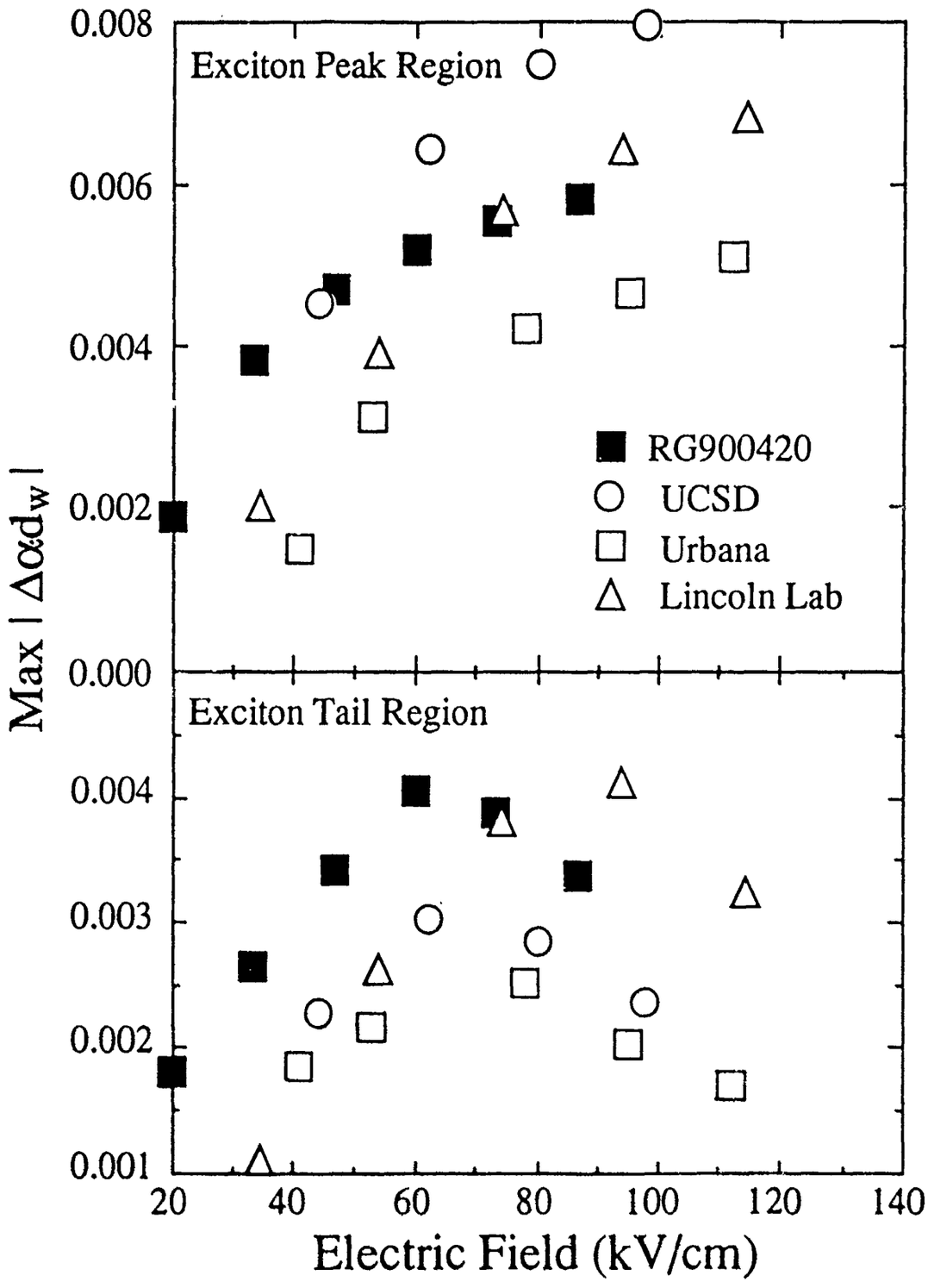
Exciton Peak Region
Exciton Tail Region
RG900420
UCSD
Urbana
Lincoln Lab
Max | Δαd_w |
0.008
0.006
0.004
0.002
0.000
0.004
0.003
0.002
0.001
20
40
60
80
100
120
140
Electric Field (kV/cm)

Fig. 17

the desired goal for low-drive voltage modulators - the absorption modulation in the exciton tail region - the region of choice for operation of the modulator - is the largest in our sample. Details of these studies may be found in **publications 13, 14, 15, 19, and 28**. It is perhaps worth noting that the basic studies of growth optimization via RHEED and feedback from the electroabsorption behavior of thick strained MQWs undertaken under this grant were put to good use for applications to asymmetric Fabry-Perot spatial light modulators needed for the projects undertaken for the USC URI on Integration of Optical Computing. Without the studies carried out under this grant the applications oriented work for the URI would not have been possible.

: Defect Reduction in Thick Strained MQWs via Patterned Growth

In addition to the defect reduction and strain variation in single layers of $In_XGa_{1-X}As$ grown on pre-patterned substrates described above, we examined the growth of $GaAs/In_XGa_{1-X}As$ multiple quantum well (MQW) structures on pre-patterned substrates. Since the underlying application oriented motivation in this case derives from use as optical modulators, two aspects of such growths are quite different from the single $In_XGa_{1-X}As$ layer structures discussed above; (1) the total thickness of the MQWs examined has ranged from 1 μm to 2.5 μm, the thickness regime required to obtain sufficient optical interaction path length for applications in light modulation devices based upon the quantum confined Stark effect and the Wannier-Stark localization effect, and (2) the pre-patterned mesas are now rectangular or circular (as opposed to stripes) with linear dimensions varying from 10 μm to 280 μm. The currently envisioned pixel size in a 2-D array of modulator pixels constituting a spatial light modulator (SLM) ranges from 10 μm to 30 μm linear dimension.

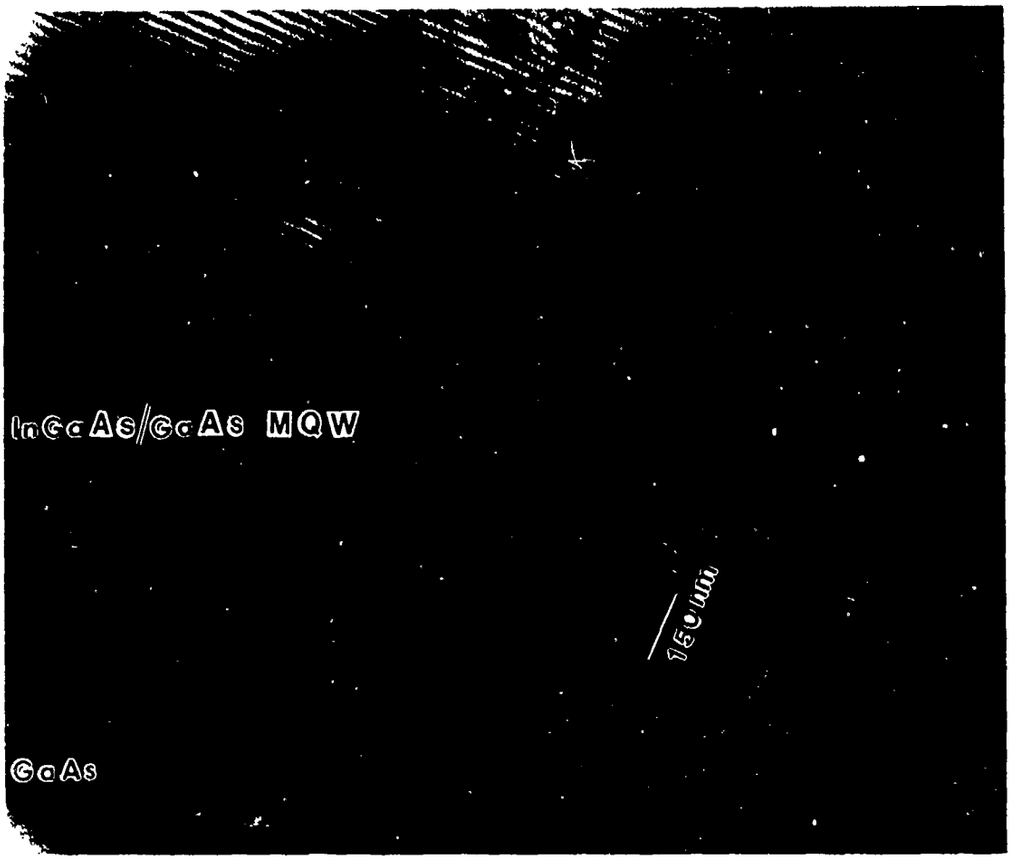

Fig. 18(a) : Shows cross-sectional TEM image of the MQW in the nonpatterned region of the GaAs (100) substrate.

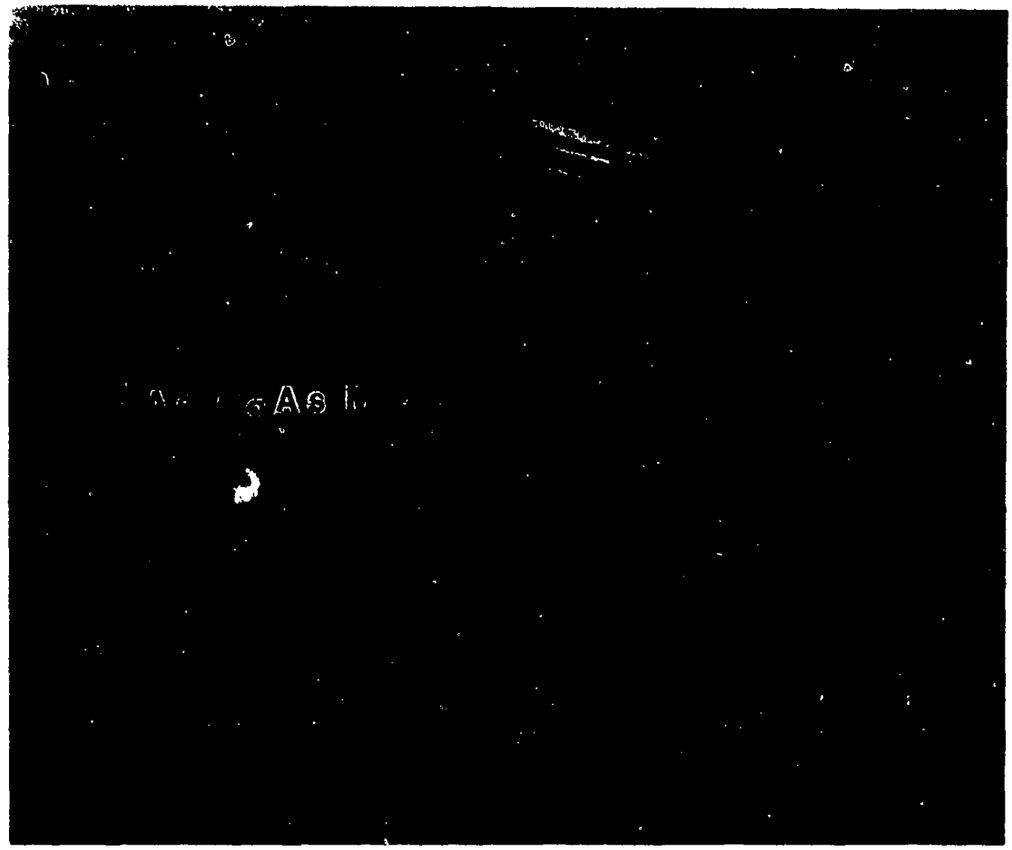

Fig. 18(b) : Shows cross-sectional TEM image of the MQW in the central region on top of the prepatterned mesas.

Fig. 18(c) : Shows cross-sectional TEM image of the MQW in the central region of the valley between the prepatterned mesas.

An illustrative example of the possible advantages in the optical properties resulting from growth of highly strained thick MQWs on pre-patterned mesas is represented by the behavior of sample RG 891110. It contains 100 periods of 80 A $In_{0.2}Ga_{0.8}As$ well and 160 A GaAs barrier layers for a total thickness of ~2.4 μm grown on a GaAs(100) substrate containing 16 μm x 18 μm rectangular mesas on 40 μm pitch and, for reference, a nonpatterned region as well. Fig. 18(a) shows a cross sectional TEM image contrast of the nonpatterned regime and, as expected, a high density of threading dislocations and other structural defects is found. By contrast, the central region of the growth on mesa, shown in fig. 18(b), exhibits very high quality of layering with very low defect density ($<10^3$/cm). Fig. 18(c) shows the TEM image contrast taken from the region between the mesas. At the level of TEM resolution ($\leq 10^3$/cm) this region (referred to as the valley region) shows no discernible difference as compared to the meas top. This in itself is surprising for one would have expected a higher defect density, though perhaps not as high as the nonpatterned region. In fig. 19 is shown the optical absorption behavior of the three regions. While no excitonic features are observed in the nonpatterned region (panel a), consistent with the high density of non-radiative recombination centers implied by the high dislocation density of fig. 18(a), the mesa top (panel b) and valley (panel c) regions show good excitonic features. What is a surprising feature is that the valley region exciton absorption (fig. 19c) is significantly sharper than for the mesa top region and the 6 meV linewidth is comparable to the best photoluminescence linewidth at 20% In composition found in *single* quantum wells. Given that this work constituted the first demonstration of the improvement in a physical property of strained MQWs by exploiting the notion of growth on pre-patterned substrates, the initial results were reported in **publication 9**.

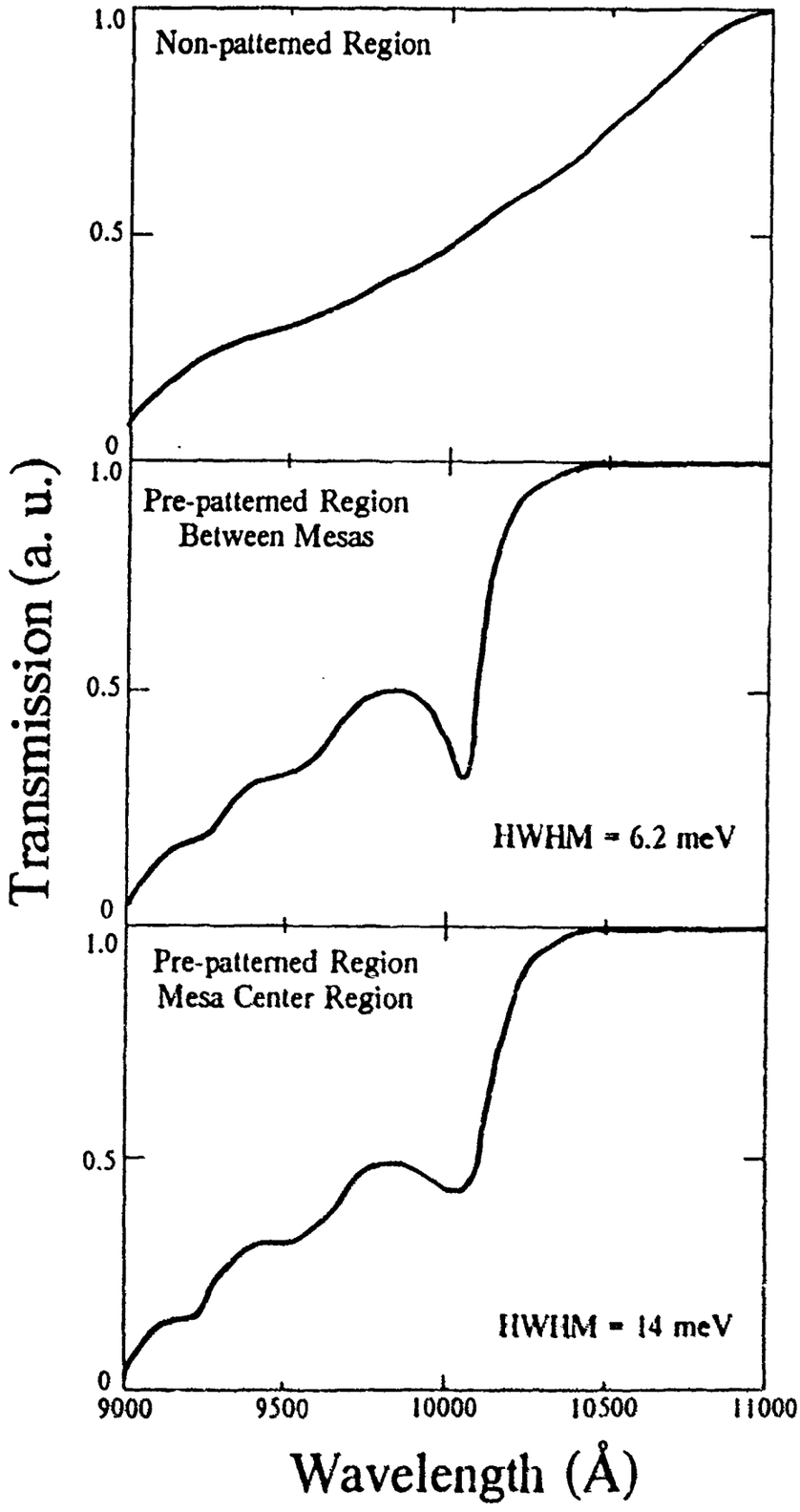
Non-patterned Region
Pre-patterned Region
Between Mesas
HWHM = 6.2 meV
Pre-patterned Region
Mesa Center Region
HWHM = 14 meV
Transmission (a. u.)
Wavelength (Å)
1.0
0.5
0
9000
9500
10000
10500
11000

Fig. 19

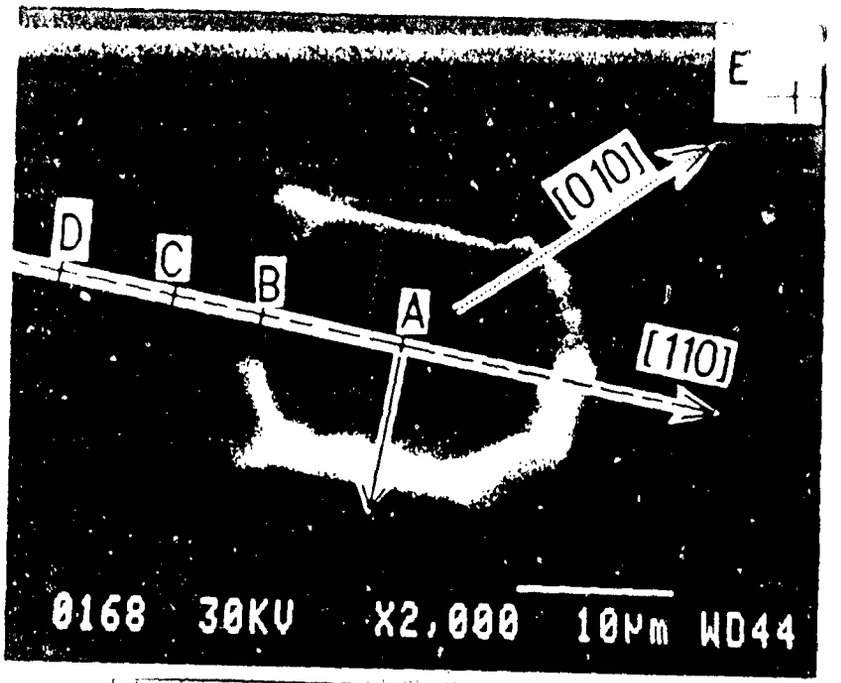
E
[010]
D
C
B
A
[110]
0168 30KV X2,000 10µm WD44

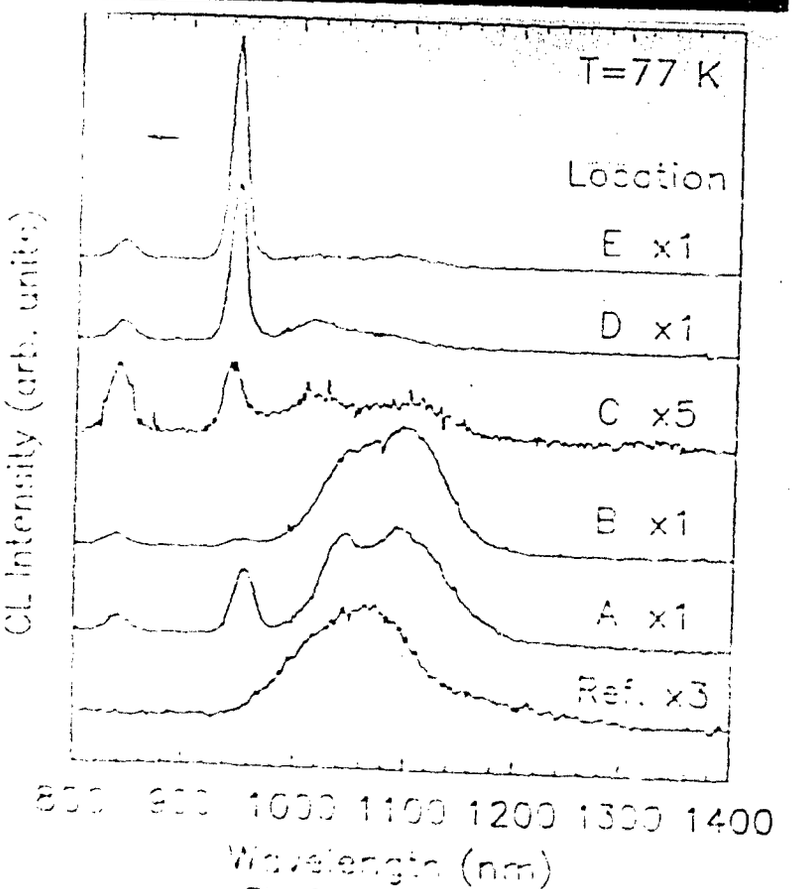
T=77 K
Location
E x1
D x1
C x5
B x1
A x1
Ref. x3
CL Intensity (arb. units)
800 900 1000 1100 1200 1300 1400
Wavelength (nm)

Fig. 20

To examine further the above noted unanticipated result, a new line of investigation was initiated with particular emphasis on obtaining a correlation between the nature and spatial distribution of the defects and the optical properties. Spatially resolved cathodoluminesence studies were thus carried out in collaboration with Prof. Daniel H. Rich (USC), even though such studies were not explicitly noted in the original research program. However, Prof. Rich's arrival at USC in Aug. '91 provided this valuable and needed opportunity. The CL results not only confirmed the earlier TEM and absorption based findings but, more importantly, showed a correlation with long wavelength (1 μm to 1.4 μm) defect related emission (see Fig. 20). We have suggested that vacancies and other point defects left in the wake of dislocation glide could be responsible for this long wavelength luminescence. These findings are reported in **publications 36 and 37**. Further investigations are continuing.

I.4. EFFECT OF SOME PROCESSING STEPS ON STRAINED QUANTUM WELLS

: Si_3N_4 Dielectric Encapsulation

As noted in sec.I.3, the as-grown single quantum well structures bearing InGaAs alloy well and binary compound (GaAs) or alloy ($Al_yGa_{1-y}As$) barrier layers have given low temperature (5K) PL linewidths as narrow as 5.1 meV for a 145A wide $In_{0.26}Ga_{0.74}As$ well sandwiched between $Al_{0.7}Ga_{0.3}As$ alloy barriers. These are amongst the narrowest linewidths achieved for simultaneously high In and Al bearing structures. Deposition of a Si_3N_4 encapsulation layer (via plasma enhanced chemical vapor deposition) was found to induce a blue-shift in the as-grown exciton position. An illustrative example is shown in fig.21. The as-grown structure is an asymmetric SQW comprised of a 145A thick $In_{0.26}Ga_{0.74}As$ well sandwiched between GaAs (lower) and AlAs (upper) barriers on which 2000A of PECVD Si_3N_4 layer was subsequently

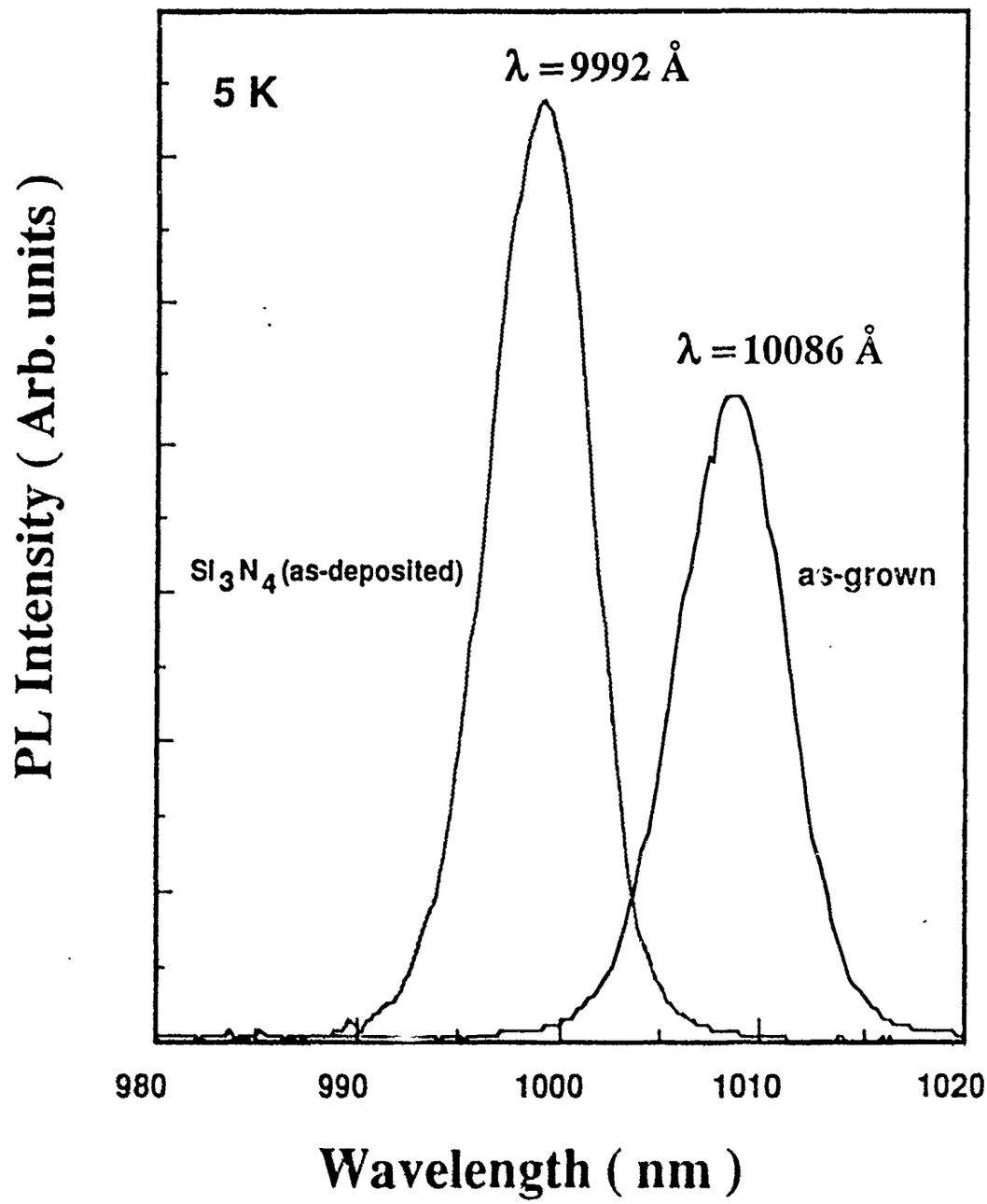
5 K
λ = 9992 Å
λ = 10086 Å
Si3N4 (as-deposited)
as-grown
PL Intensity (Arb. units)
980
990
1000
1010
1020
Wavelength (nm)

Fig. 21

deposited. An exciton blue shift of 94A is observed. The dielectric induced blue shift was observed to be a general feature although the magnitude of the shift is naturally dependent upon the specific structure and, to some extent, the Si_3N_4 deposition conditions. The exciton peak shift indicates that the Si_3N_4 induces a further strain in concert with the strain already present in the as-grown structure. From the view point of device design the dielectric induced exciton shifts found in these studies caution one to account for such effects. Further details may be found in **publication 35**.

: Rapid Thermal Annealing

Under this grant some studies of rapid thermal annealing (RTA) of both the as-grown and Si_3N_4 encapsulated SQW structures were initiated. For both types of samples, RTA was found to induce a major blue-shift in the exciton although the shifts were smaller for the Si_3N_4 encapsulated structures. As an illustration, fig. 22 shows the results for a SQW comprised of a 160A thick $[(In_{0.35}Ga_{0.65}As)_{15}$ / $(GaAs)_4]_3$ layer as the well, GaAs as the lower barrier, and $[(AlAs)_5$ / $(GaAs)_2]_{13}$ short period multiple quantum well as the upper barrier layer. At each RTA temperature shown, both the as-grown and Si_3N_4 encapsulated specimens were exposed to RTA for 6 sec. under ultra high pure N_2 environment. While the exciton blue shifts for the unencapsulated specimen are truly dramatic, they are nevertheless significant for the encapsulated specimen. We take the view that these blue shifts are indicative of cation interdiffusion across the interfaces, particularly at the GaAs/InGaAs interface at the lower barrier, induced in the strained metastable structures upon RTA. Such interdiffusion will change the nature of the as-grown quantum well confining potential as illustrated in fig.23, thus giving rise to a blue shift in the exciton

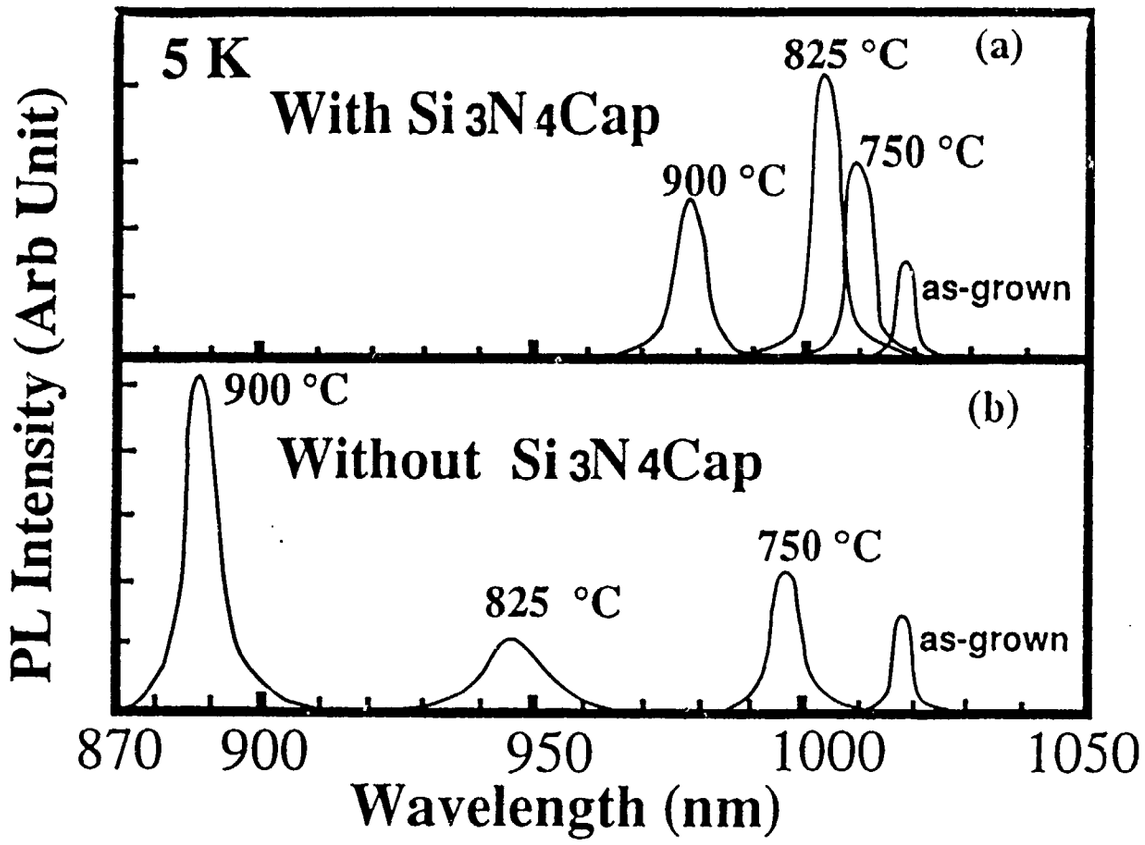
5 K
With Si 3N 4Cap
825 °C
(a)
900 °C
750 °C
as-grown
900 °C
(b)
Without Si 3N 4Cap
750 °C
825 °C
as-grown
PL Intensity (Arb Unit)
870
900
950
1000
1050
Wavelength (nm)

Fig.22

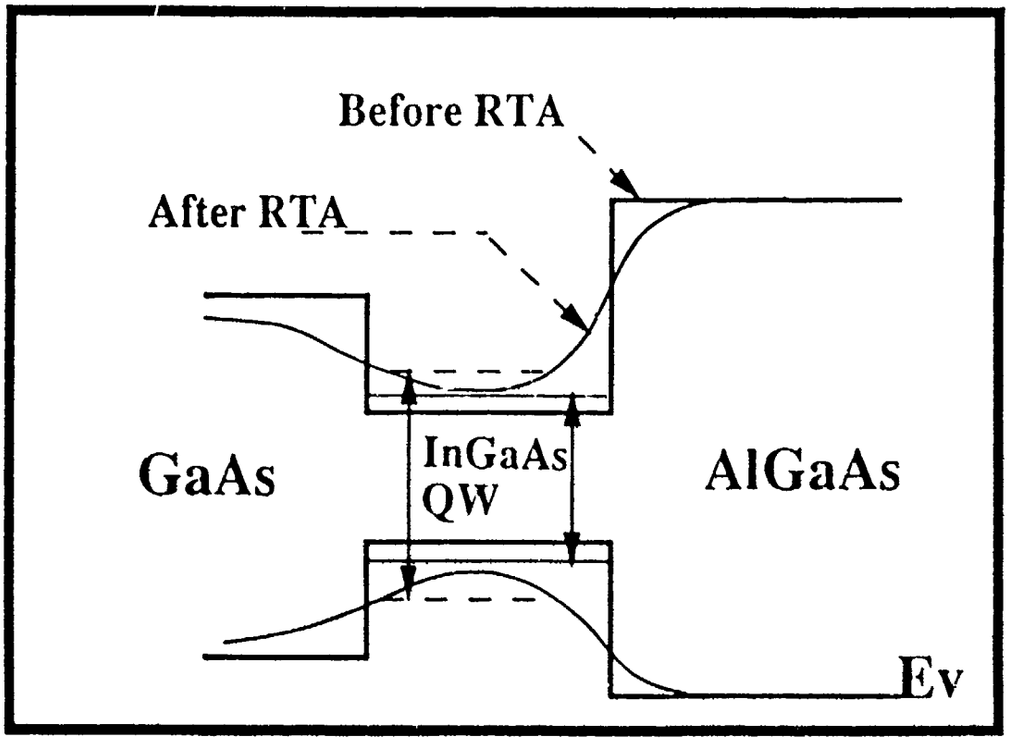
Before RTA
After RTA
GaAs
InGaAs
QW
AlGaAs
Ev

Fig.23

position. Within the resources of this grant, this point could not be pursued further. Fortunately other sources allowed some further examination of our proposed view via theoretical modelling. Results obtained with support from this grant were reported in **publication 35**. Further details, including theoretical modelling can be found in K. Kaviani, Ph.D. Dissertation, University of Southern California, 1993.

I.5. REALIZATION OF 3-DIMENSIONALLY CONFINED STRUCTURES VIA ONE-STEP GROWTH ON APPROPRIATELY PATTERNED MESAS

: Pyramidal Boxes with Triangular Base on GaAs(111)B

As noted in Sec. I.1, etching of GaAs(111)B gives pyramidal mesas with triangular (111)B mesa tops bounded by {100} type three side planes (see Fig. 24). The linear dimension of the triangular mesa top is determined by the duration of the etch. Such triangular pyramidal mesas afford the opportunity of realizing, via purely growth control, 2-dimensional arrays of 3-dimensionally confined structures. Since this is an *in-situ* process, patterning and/or etching related damage and contamination is avoided. The *in-situ* approach thus holds the promise of realizing structures with lateral dimensions in the quantum confinement regime but without compromising the electronic and optical properties. A large part of our effort was focussed on examining this tantalizing possibility. Its realization is predicated upon finding growth conditions whose operative growth kinetics are such as to give rise to monotonic reduction in the (111)B triangular mesa top dimensions with continued growth. In other words, growth conditions such that associated interfacet migration involves movement of atoms into the (111)B mesa tops. That this is possible was demonstrated in 1987-88 for the first time in our AFOSR supported work on the growth on patterned GaAs(100) substrates which contain (100) mesa tops contiguous with

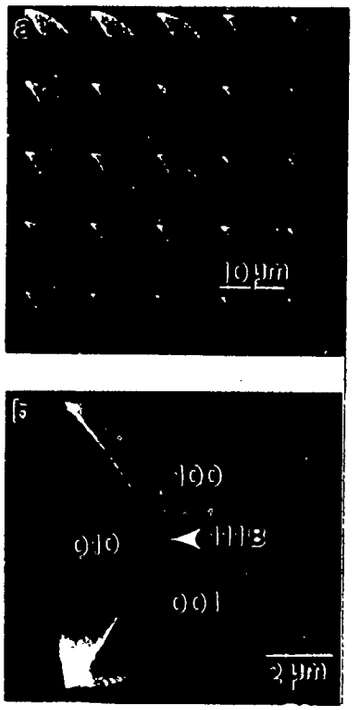

Fig. 24

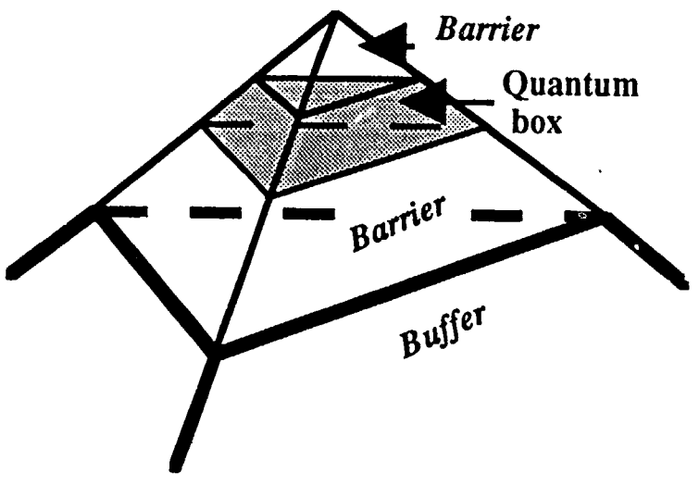

Fig. 25

(111) sides walls in the as-patterned condition. Thermal treatment of such as-patterned substrates under appropriate arsenic flux in the MBE growth chamber was shown, via marker layer high resolution TEM experiments, to lead to the formation of (211)/(311) type facets between the (100) mesa top and (111) mesa sidewalls. The presence of such facets was shown to give rise to migration of adatoms during growth to the (100) mesa top *and* (111) mesa sidewalls. This included growth conditions such that rapid interfacet migration led to no growth on the (311) type sidefacets. Guided by these earlier findings, systematic studies were undertaken to find the appropriate growth conditions for growth on (111)B mesa tops such that a laterally shrinking mesa top growth profile would result and permit realization of a quantum box as schematically shown in Fig. 25.

While **publications 38, 40, and 41** provide more detail, here we briefly note the highlights of this effort. Through systematic exploitation of RHEED controlled growth conditions we have succeeded in achieving mesa top growth profiles ranging from continually expanding, to initially expanding and subsequently contracting, to monotonically contracting during growth. The lattermost is the desired situation for achieving 3-dimensionally confined structures. GaAs/$Al_{0.3}Ga_{0.7}As$ quantum wells with lateral dimensions ~325°A and a height of 65°A (containing ~5.8 x 10^4 atoms) have been realized on as-patterned starting mesa sizes ~ 0.6 μm. Indeed, the greatest difficulties faced in achieving uniformity in the 2-D array and in reproducibility arise from two *extrinsic* effects: (i) uniformity and reproducibility of the as-patterned mesa sizes on the starting substrate - a consequence of the wet chemical etching induced variations, and (ii) geometrical effects relating the MBE growth chamber cell configuration in relationship to the substrate orientation. Note that the 3-fold symmetry of the pyramidal mesas presents issues of flux uniformity on individual mesa side facets which are not faced for growth on planar substrates. In the

Fig. 26

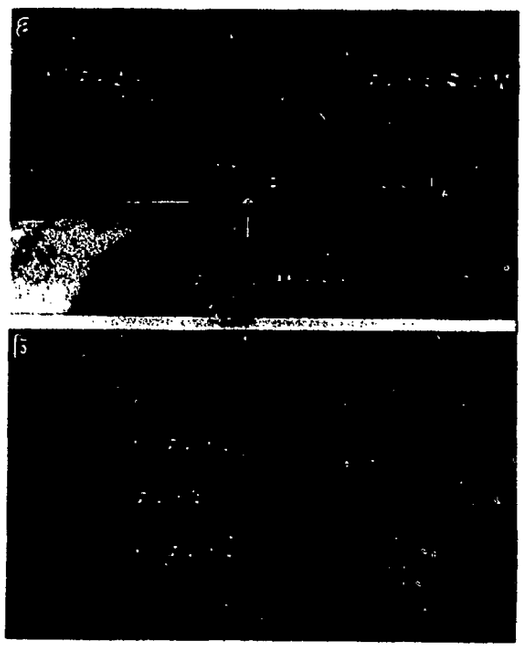

Fig. 27

following we show a few illustrative results corresponding to stabilization of two different types of side-facets, {211} and {110}, achieved via control on growth kinetics.

Two illustrative results - one for a GaAs (40 ML) / $Al_{0.3}Ga_{0.7}As$ (10 ML) 13 period coupled quantum well and the other for a 40 ML GaAs single quantum well sandwiched between $Al_{0.3}Ga_{0.7}As$ barrier layers - are shown in Figures 26 and 27, respectively. The figures are (200) dark field image contrast taken along the <110> azimuth in a transmission electron microscope. The emergence of (211) side facets and the shrinking nature of the (111)B mesa top growth profile are clearly seen. Photoluminescence studies on these samples show clear and intrinsic excitonic lines (as determined via temperature and incident power dependence), thus confirming the value of *in-situ* growth approach in avoiding the damage and contamination caused in post-growth patterning/etching approaches. However, no quantum confinement induced shifts in the excitonic lines were seen nor were expected given that the lateral dimensions of the 3-D confined quantum well structures in these samples are still greater than 2500 Å. For completeness we parenthetically note that the TEM studies on these samples were carried out under other support. These results were reported at the MRS Spring Meeting (April 27 - May 1, 1992 in San Francisco) and are given in **publication 38**.

While further work (publications 40 and 41) on the realization of GaAs(111)B based pyramidal volumes under growth kinetics that stabilize {211} sidefacets as in fig. 26 allowed achieving lateral dimensions as small as ~500°A, the luminescence properties of such volumes were found to be compromised by the tunnelling of the electrons and holes out of the box due to insufficient lateral barrier height provided by the electron and hole levels in the thinner but nonzero well widths on the {211} sidewalls. Ideally one would like the absence of the well

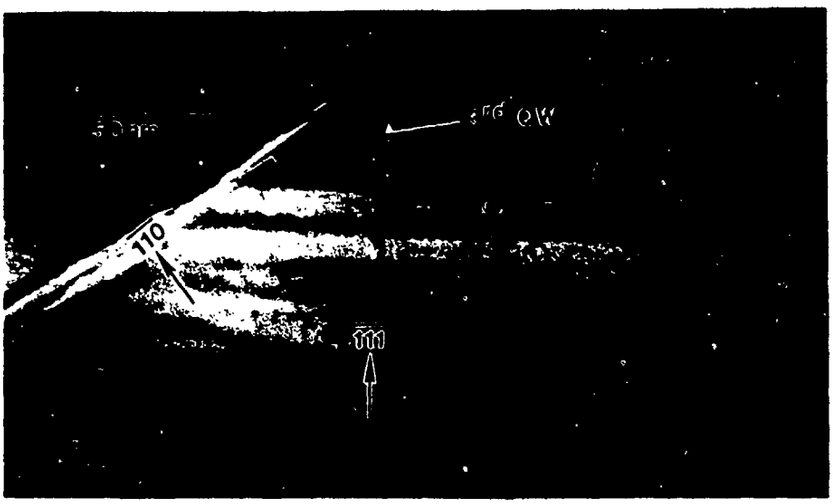

Fig. 28

layer growth on the side walls of the 3-dimensionally confined volume so that the growth of the barrier material provides the largest possible lateral barriers and hence the strongest possible lateral confinement. With this objective in mind we explored other regimes of growth kinetics and uncovered appropriate regimes in which {110} sidewalls are stabilized (as opposed to {211}) with no growth of the GaAs well layers on the {110} sidewalls. An example of such growth is shown in fig. 28. This sample consisted of the deposition of four GaAs wells of thickness 20ML (for unpatterned growth) sandwiched between 40ML $Al_{0.3}Ga_{0.7}As$ barrier layers, once the as-patterned mesa of linear dimension 0.6μm had been reduced in size by the growth of GaAs buffer layer marked with 5ML thick $Al_{0.3}Ga_{0.7}As$ marker layers every 46ML of GaAs deposition. In the XTEM picture of fig. 28 the first three wells are clearly seen, the 4th and topmost are beign absent as, regretably, during the TEM specimen preparation the mesa top region got milled away. The linear dimensions of the base and the top of the 3rd quantum well in fig. 25 are 1116°A and 716°A, respectively and the thickness is 84°A. Given these dimensions and the {110} sidewall orientation, we can reliably calculate that mesa pinch-off occurred in the 4th deposited well as intended and that the linear dimension of this 3-dimensionally confined volume is 324°A and the height 65°A. Such dimensions are in the regime of quantum confinement of the electronic states and the quantum box contains ~ 5.8×10^4 atoms.

To examine the optical quality of such samples, we undertook collaborative studies with Prof. Daniel Rich (USC) using spectrally- and spatially-resolved cathdoluminescence. Fig. 29 shows the spectral behavior for the emissions from the reference unpatterned area and from the mesa region. The 812nm and 789nm emissions in the former correspond to the GaAs buffer and the four 20ML thick quantum wells. (The calculated value for the 20ML thick quantum wells is 789.5nm). For the mesa region, spatial imaging with the

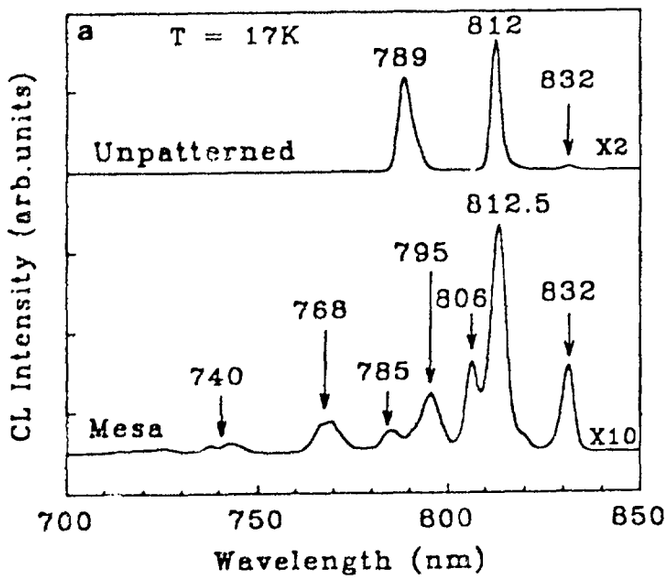
a
T = 17K
789
812
832
Unpatterned
X2
812.5
795
768
806
832
740
785
Mesa
X10
CL Intensity (arb.units)
700
750
800
850
Wavelength (nm)

Fig. 29

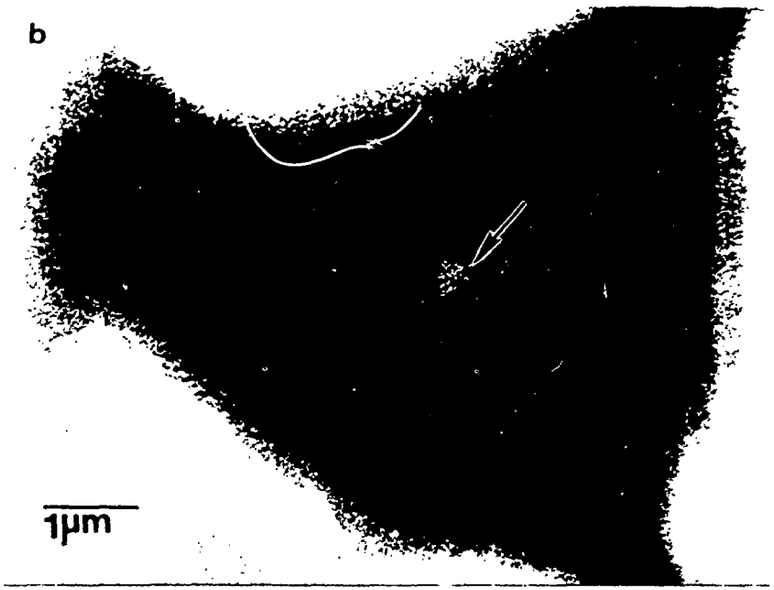
b
1μm

Fig. 30

observed emission lines showed that all except the 812.5 nm and 795nm emissions originate from regions other than the mesa top. The 812.5 nm emission is from the buffer layer on the mesa top and the correspondence with the emission from the buffer layer in the unpatterned region is expected. The 795nm emission if from the first three quantum wells grown on the mesa top and the red shift with respect tothe 789nm emission from the unpatterned region wells is a combined consequence of (a) the mesa top well layers begin thicker (24ML to 26ML) than the unpatterned region (20ML) due to the migration of the atoms from the {110} sidefacets to the mesa top, and (b) the lateral linear dimensions of these three wells being >716°A so that no lateral confinement (and hence a blue shift in the emission) is expected. The 4th and topmost well constitutes a true 3-dimensionally confined volume in the quantum box regime of lateral size and thus, at face value, might have been expected to exhibit emissions at a wavelength shorter than 795nm. However, no unambiguous indication of the presence of such a peak is observed in the emission spectrum. We believe this is a combined consequence of the fast tunnelling rate out of the box for the electrons (and probably holes) due to the vertical confining $Al_{0.3}Ga_{0.7}As$ barrier layer not being thick enough, the availability of lower energy levels in the three wells below the quantum box, and the small excitation volume of the box. Improved vertical confinement requires thicker AlGaAs barrier layers and preferably deposition of a single well. Efforts in this direction are continuing. Finally, a spatial image of the mesa region taken with the 795nm emission is shown in fig. 30. The emission is seen to originate in the mesa top region. These results are to be published (**publication 46**).

: **Pyramidal Boxes with Square Base on GaAs(100)**

In the preceding we summarized the highlights of the work accomplished on the creation of quantum box structures via growth on GaAs(111)B triangular base mesas. The choice of the GaAs(111)B surface was motivated by recognition of two facts, (i) all previous work, largely motivated by ridge lasers, on long mesa stripes patterned along <011> directions on GaAs(100) substrates had indicated that during MBE growth mesa top size-reduction occurs either only for stripes patterned along the $[0\bar{1}1]$ direction or if it ocurs for the orthogonal patterning direction [011] then the rate of mesa top size-reduction is not the same as for the $[0\bar{1}1]$ oriented mesa stripes. Thus the two types of side facets present are not equals and conventional patterning along <011> directions is at best suitable for the realization of quantum wires on the mesa tops, as first demonstrated in our AFOSR sponsored work in 1987-88. While these known facts of nearly a decade raise the fundamental question of in what sense are the two mutually orthogonal <011> patterning directions not equivalent and why does size reduction occur readily for only the $[0\bar{1}1]$ patterning direction, they do suggest that for achieving equal size-reduction from all lateral sides that is necessary for the realization of 3-dimensionally confined structures, one must look for starting mesas with equivalent side facets, (ii) the triangular base pyramidal mesas on GaAs(111)B offer 3-fold symmetry due to the equivalent {110} sidewalls and hence can potentialy give equivalent interfacet migration from the sidewalls to the mesa to, thus leading to equal rate of size reduction from all sides and hence quantum boxes as demonstrated in the preceding.

Under this grant then, another issue we addressed is the issue of the underlying atomistic and kinetic reason for the particular behaviorof interfacet migration for <011> oriented mesas on GaAs(100) and whether or not the answer to this long standing unexplained behavior might provide the clue for finding appropriate mesa orientation on GaAs(001) that lends itself to equal mesa

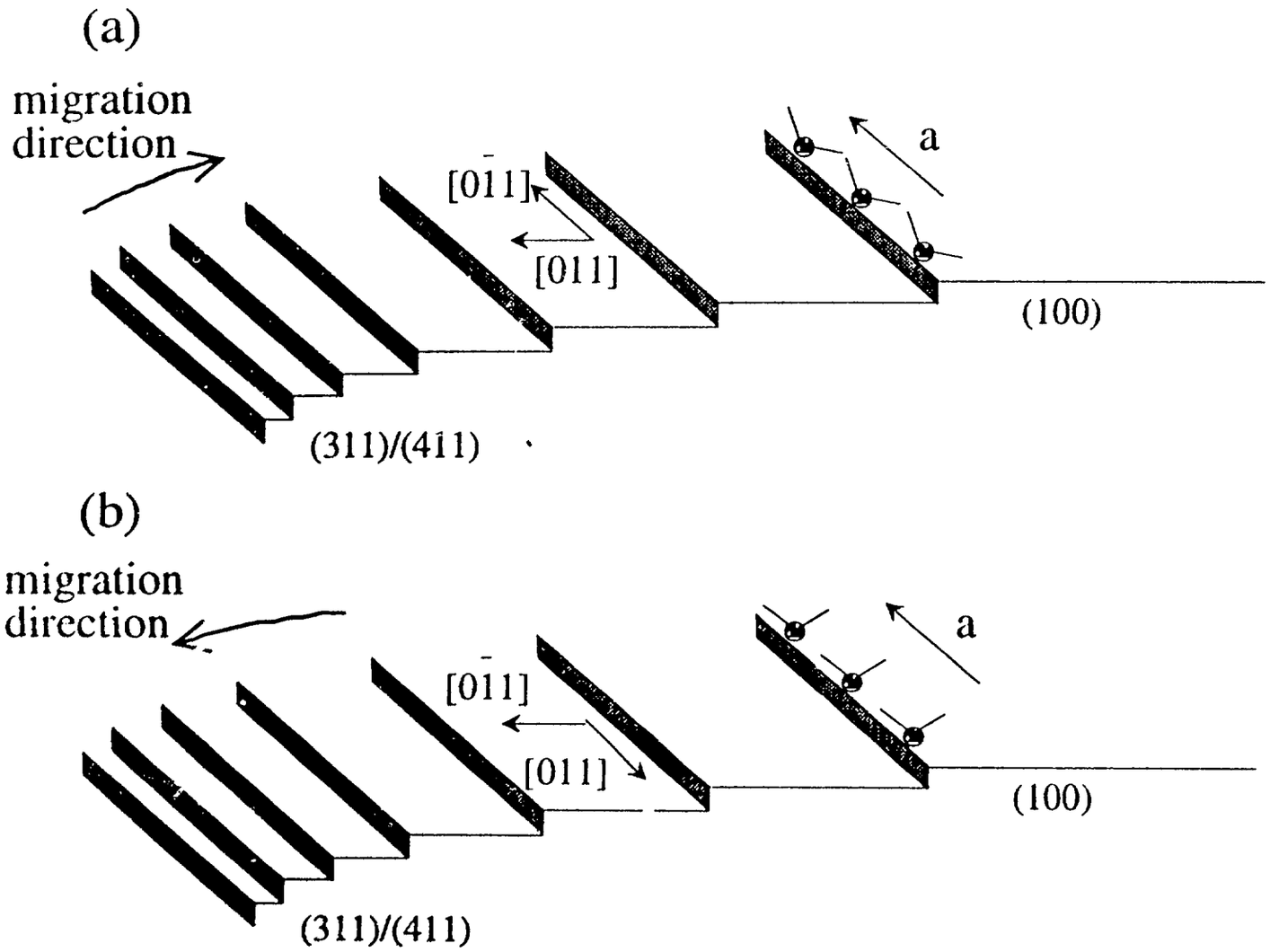
(a)
migration
direction
[0$\bar{1}$1]
[011]
a
(100)
(311)/(4$\bar{1}$1)
(b)
migration
direction
[0$\bar{1}$1]
[011]
a
(100)
(311)/(4$\bar{1}$1)

Fig. 31

top size reduction from all sides and hence to the realization of quatum boxes. An explanation was found in the direction of orientation of the dangling orbitals of the surface atoms with respect to the mesa edges as shown in fig. 31. For the case of the patterning direction [$0\bar{1}1$], fig. 31(a), the arsenic dangling orbitals are parallel to the mesa edge whereas for the orthogonal [011] direction, fig. 31 (b), they are perpendicular to the mesa edge. In the former case, migration is seen to occur fro the {311}/{411} type sidewalls generally found to the mesa top, a direction that is opposite to the direction of concentration gradient due to vapour flux incident normally to the GaAs(100) mesa top in usual MBE growth. Such interfacet migration against the concentration gradient can occure only if there were directed driving force opposing the concentration gradient since we had earlier demonstrated experimentally that the sticking coefficient of the group III atoms is unity on the sidewalls under the MBE growth conditions employed. For the latter case (fig. 31b) the observed migration is from the meas top to the sidewall, the same as the direction of concentration gradient during growth and the mesa top is observed to expand, not shrink as desired for quantum box realization. For the origin of a directed force that competes with the random thermal forces and concentration gradient, we have identified the step-step interaction arising from the stress fields associated with the steps present on the sidewalls, as shown schematically in fig. 31. Molecular dynamics based calculations of the step-step interaction energies for steps on GaAs(100) first carried out by Choi et al in the group of Prof. W. Tiller of Stanford and subsequently independently confirmed in our own calculations show that these energies increase (decrease) with increasing step separation for the case of As orbitals parallel (perpendicular) to the mesa edge. For the parallel case they thus provide a driving force opposite to the concentration grandient line (i.e. from the sidewalls to the top) whereas for the perpendicular case they provide a driving

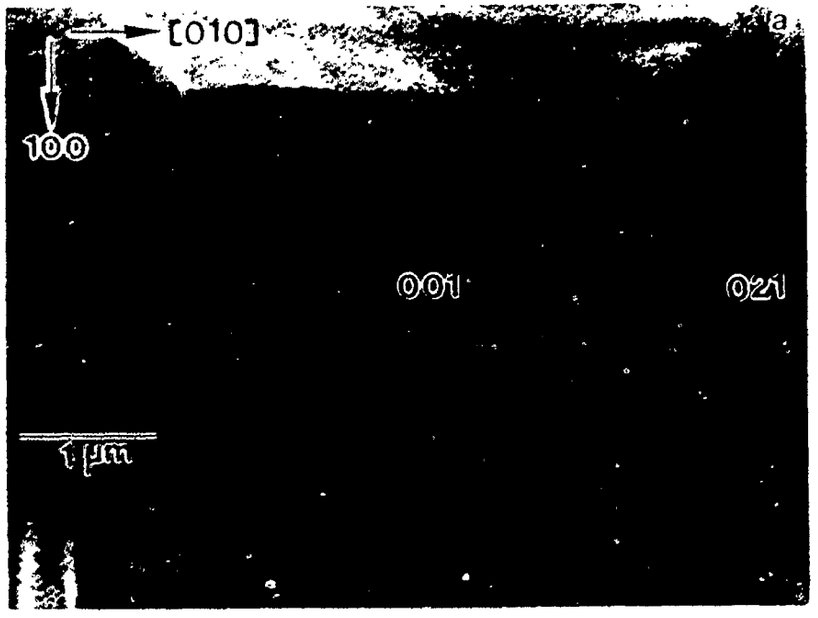
[010]
100
001
021
1μm

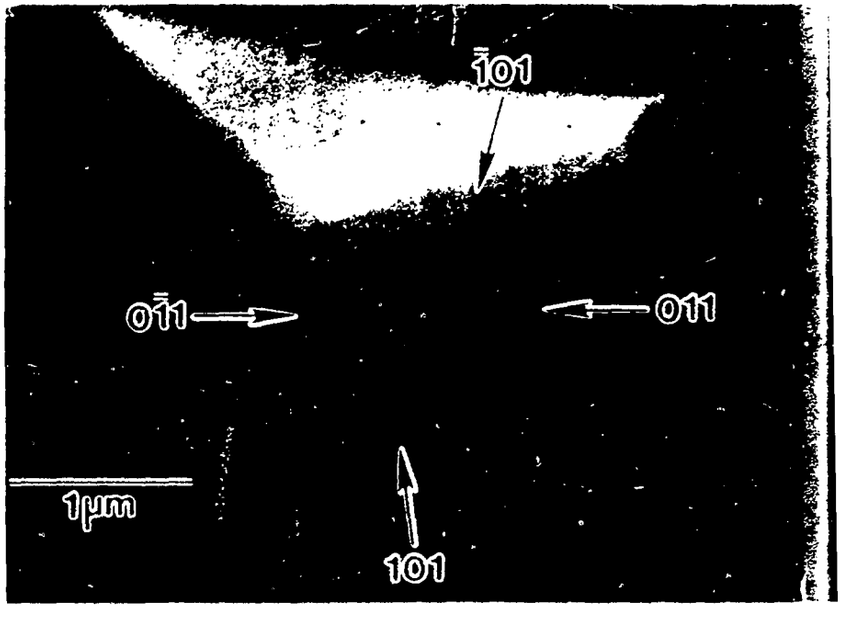
$\bar{1}01$
$0\bar{1}1$
011
1μm
101

force in the same direction as the concentration gradient (i.e. from the mesa top to the sidewalls). This atomistic understanding and a kinetic explanation was first offered by us in S. Guha's Ph.D. dissertation (University of Southern California, 1991) and was subsequently reported in **publication 45**. This explanation brings to fore the fundamental significance of electronic and lattice interaction energies in controlling the net kinetics of surface migration and introduces the idea of Substrate Encoded Size-Reducing Eptitaxy (SESRE) i.e. the notion that size-reduction can be encoded into the starting mesa if only the choice of the mesa shape and orientation is made based upon such atomic understanding.

A natural implication of our proposed explanation of the observed directionality of interfacet migration for the conventionally chosen <011> oriented mesas on GaAs(100) and a test of the notion of SESRE then is that if the mesa orientation was chosen to be along the <010> directions then the dangling orbitals for all four mesa edges will be at the same 45° to the mesa edge and hence all four mesa sidewalls should be equivalent in their interfacet migration behavior with respect to the mesa top. Consequently, to realize 3-dimensionally confined structures on GaAs(100) we undertook experimental work on growth on square mesas oriented with their edges along <010> directions. A typical mesa obtained via usual wet chemical etching is shown in fig. 32(a).

Starting with an array of mesas of the type shown in fig. 32(a), upon growth of GaAs/AlGaAs multilayered structures (in which the AlGaAs layers were placed more as marker layers for examining the growth front evolution rather than as thick barrier layers to achieve vertical confinement) we obtained mesa top size reduction leading to mesa pinch-off as seen in fig. 32(b) and 33. Having demonstrated the essential correctness of the notion of SESRE we then proceeded to realize quantum box structures comprised of GaAs surrounded on all sides by AlGaAs. A XTEM image of the region near the mesa pinch-off for

Fig. 33

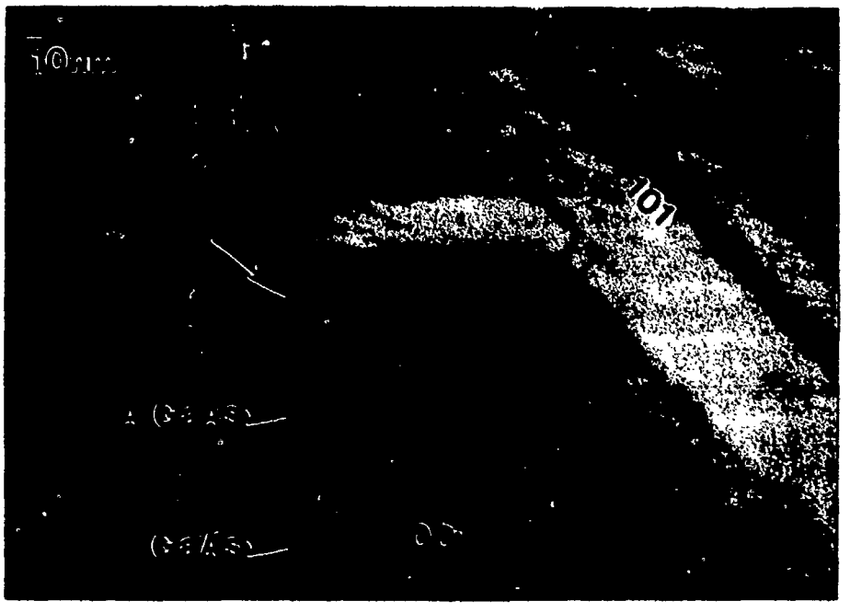

Fig. 34

one such growth is shown in fig. 34. The dark layers are GaAs and the bright layers are $Al_{0.3}Ga_{0.7}As$. The region marked by the arrow represents a GaAs quantum box with a base of 440°A, top of °A, and a height of 100°A. It contains ~ x x 10y atoms and represents the first realization of a quantum box via MBE growth on non-planar substrate. These results are yet to be published (publication 47).

I.6. IN-SITU, DIRECT WRITE, FOCUSED ION BEAM PATTERNING OF GaAs(100)

During this grant period we received, installed, and tested a custom designed UHV focussed ion beam system, UHV interconnected to our MBE growth system. This system was largely acquired with supplemental equipment funds provided earlier by the AFOSR. Consequently we provide a brief report on the studies conducted with this system.

While ion-solid interaction is a subject with a long history, the semiconductor related work has largely been devoted to high energy (> 100 KeV) ions. The use of relatively lower energy ions (< 25 KeV) in FIB studies is a relatively newer phenomenon. As such, little by way of systematic studies in general, and that for Ga^+ FIB in GaAs in particular, existed. Consequently we devoted a significant part of our effort to systematic studies involving variations in the relevant Ga^+ ion beam parameters (energy, current, dwell time, scan, dose, etc.) and examination of the nature of the resulting material via scanning electron microscopy (SEM), Auger electron spectroscopy (AES), transmission electron microscopy (TEM) and few other techniques. Such systematic effort could fortunately be mounted since a significant part of the graduate student manpower needed for such a comprehensive study was provided by the DARPA sponsored National Center for Integrated Photonic Technology (NCIPT). Thus a significant

leveraging of the AFOSR investment in the instrument and operation was provided by the significant operational support under NCIPT.

Of the variety of situations examined, we summarize here the essentials of our findings on two aspects: (i) the formation of Ga droplets in sputtering of GaAs, and (ii) Ga^+ FIB assisted Cl_2 etching of GaAs. It had been observed by others that Ga^+ FIB of Si and GaAs gives rise to formation of Ga droplets when attempts are made to obtain sputtering (i.e. milling) with the objective of direct-write patterning. Since this could be a compromising factor in the potential use of FIB patterning, we undertook systematic examination to reveal and understand the nature of the Ga droplet formation process. The essential findings established for the first objective are as follows;

(i) Ga droplet formation occurs beyond a threshold dose of ~ $2 \times 10^{16}/cm^2$, independent of the beam conditions.

(ii) Ga droplet formation begins when the excess Ga concentration in the subsurface region reaches ~ 32%.

(iii) The Ga droplet formation is driven by the instantaneous energy deposited by the energetic ions at the surface. It is thus a highly non-equilibrium process, not simply a consequence of the local heating effect.

(iv) The Ga droplet cluster size distribution is dependent upon the ion beam current employed for the same total dose.

These and other results were reported at the MRS Spring Meeting (April 27 - May 1, 1992) in San Francisco and may be found in **publication 39**.

II. LIST OF PUBLICATIONS

(Note: Publications 1 through 8 represent work essentially completed under prior AFOSR grant but published during this grant period.)

1. S. Guha, A. Madhukar, K. Kaviani, R. Kapre, "Growth of $In_xGa_{1-x}As$ on Patterned GaAs(100) Substrates", Jour. Vac. Sc. Tech. B8, 149 (1990).

2. A. Madhukar, "The Nature of Molecular Beam Epitaxy and Consequences for Quantum Microstructures" in Topics in Applied Physics, "Physics of Quantum Electron Devices" (Ed. F. Capasso), Springer Publications, Vol. 28, p.13 (1990).

3. D.J. Kim, A. Madhukar, K.Z. Hu, W. Chen, "Realization of High Mobilities at Ultra Low Electron Density in $GaAsAl_{0.3}Ga_{0.7}As$ Inverted Heterojunctions", App. Phys. Lett. 56, 1874 (1990).

4. R. Kapre, A. Madhukar, K. Kaviani, S. Guha and K.C. Rajkumar, "Realization and Analysis of GaAs/AlAs/$In_{0.1}Ga_{0.9}As$ Based Resonant Tunneling Diodes with High Peak to Valley Ratios at Room Temperature, App. Phys. Lett. 56, 922 (1990).

5. S. Guha, A. Madhukar and Li Chen, "Defect Reduction in Strained $In_xGa_{1-x}As$ via Growth on GaAs(100) Substrates Patterned to Submicron Dimensions", App. Phys. Letts. 56, 2304 (1990).

6. S. Guha, A. Madhukar, Li Chen, K.C. Rajkumar and R. Kapre, "Interfacet Migration and Defect Formation in Heteroepitaxy on Patterned Substrates: AlGaAs and InGaAs on GaAs(100) in MBE", SPIE Proceedings on "Growth of Semiconductor Structures and High T_C Superconductors", Ed. A. Madhukar, Thin Films on Semiconductors, 1285, 160 (1990).

7. P.M. Echternach, Kezhong Hu, A. Madhukar, H.M. Bozler, "Transport Measurements on a High Mobility, Ultralow Carrier Concentration Inverted GaAs/AlGaAs Heterostructure", Physica B (N. Holland) 165/166, 871 (1990).

8. K. Pastor, M. Goiran, D.J. Kim, A. Madhukar, J. Leotin, M. Bouchelaghem and S. Askenazy, "Effect of Inhomogeneous Charge Distribution on the Cyclotron Resonance in Inverted $GaAs/Ga_{1-x}Al_xAs$ Interface" Proceedings of the 20th International Conference of the Physics of Semiconductors, (Aug. 1990, Tessaloniki, Greece), Eds. E.M. Anastassakis, J. Joannopoulos, (World Scientific, Singapore) 2, 1365 (1990).

9. A. Madhukar, K.C. Rajkumar, Li Chen, S. Guha, K. Kaviani and R. Kapre, "Realization of Low Defect Density, Ultra Thick, Strained InGaAs/GaAs Multiple Quantum Well Structures via Growth on Patterned GaAs(100) Substrates", App. Phys. Letts., 57, 2007 (1990).

10. S. Guha, A. Madhukar and K.C. Rajkumar, "Onset of Incoherency and Defect Introduction in the Initial Stages of Molecular Beam Epitaxical Growth of Highly Strained $In_xGa_{1-x}As$ on GaAs(100), App. Phys. Letts. 57, 2110 (1990).

11. R. Kapre, A. Madhukar and S. Guha, "$In_{0.25}Ga_{0.75}As$/AlAs Based Resonant Tunneling Diodes Grown on Pre-patterned and Non-patterned GaAs(100) Substrates", IEEE Electron Device Lett, 11, 270 (1990).

12. K.C. Rajkumar, P. Chen and A. Madhukar, "Studies of the RHEED Specular Beam Intensity Variations on MBE Grown GaAs(111)B Surface", Proceedings of the 20th ICPS Conference (Aug. 1990, Thessaloniki, Greece), Eds. E.M. Anastassakis, J. Joannopoulos, (World Scientific, Singapore), 1, 276 (1990).

13. Li Chen, A. Madhukar, K.C. Rajkumar, K. Hu and J.J. Jung, "Optical Properties of Highly Strained $In_xGa_{1-x}As$/GaAs Quantum Wells Structures Grown via MBE on Conventional and Patterned GaAs(100) Surfaces", Proceedings of the 20th ICPS Conference (Aug. 1990, Thessaloniki, Greece), Eds. E.M. Anastassakis, J. Joannopoulos, (World Scientific, Singapore) 2, 1117 (1990).

14. Li Chen, K.C. Rajkumar and A. Madhukar, "Optical Absorption and Modulation Behavior of Strained $In_xGa_{1-x}As$/GaAs(100) ($x \leq 0.25$) Multiple Quantum Well Structures Grown via Molecular Beam Epitaxy", App. Phys. Letts. 57, 2478 (1990).

15. Li Chen, K. Hu and A. Madhukar, "Behavior of Absorption Modulation in Highly Strained $In_xGa_{1-x}As$/GaAs Multiple Quantum Wells Grown via Molecular Beam Epitaxy on Patterned and Nonpatterned GaAs(100) Substrates", Mat. Res. Soc. EA-21, 317 (1990).

16. K.C. Rajkumar, P. Chen and A. Madhukar, "A Transmission Electron Microscope Study of Twin Structure GaAs/GaAs(111)B Grown via Molecular Beam Epitaxy", Jour. Appl. Phys. 69, 2219 (1991).

17. S. Guha, K.C. Rajkumar and A. Madhukar, "The Nature and Control of Morphology and the Formation of Defects in InGaAs Epilayers and InAs/GaAs Superlattices Grown via MBE on GaAs(100), Jour. Cryst. Growth, 111, 434 (1991).

18. R. Kapre, A. Madhukar and S. Guha, "Highly Strained Pseudomorphic $In_xGa_{1-x}As$/AlAs Based Resonant Tunneling Diodes Grown on Patterned and Non Patterned GaAs(100) Substrates", Jour. Cryst. Growth, 111, 1110 (1991).

19. Li Chen, K.C. Rajkumar, A. Madhukar, W. Chen, S. Guha and K. Kaviani, "Realization of Sharp Excitonic Features in Highly Strained GaAs/$In_xGa_{1-x}As$ Multiple Quantum Wells Grown on GaAs(100) Substrates", Jour. Cryst. Growth, 111, 424 (1991).

20. W.C. Tang, H.J. Rosen, S. Guha and A. Madhukar, "Raman Microprobe Study of Narrow $In_xGa_{1-x}As$ Stripes on Patterned GaAs(100) Substrates", Appl. Phys. Lett. 58, 1644 (1991).

21. P. Chen, K.C. Rajkumar, A. Madhukar, "Growth Control of GaAs Epilayers with Specular Surface Free of Pyramids and Twins on GaAs(111)B Substrates via Molecular Beam Epitaxy", Appl. Phys. Letts. 58, 1771 (1991).

22. P. Chen, K.C. Rajkumar and A. Madhukar, "Relation between Reflection High Energy Electron Diffraction Specular Beam Intensity and the Surface Atomic Structure/Surface Morphology of GaAs(111)B", Jour. Vac. Sci. Tech. B 9, 2312 (1991).

23. S. Guha, A. Madhukar, R. Kapre and K.C. Rajkumar, "Initial Stages of Molecular Beam Epitaxical Growth of Highly Strained $In_xGa_{1-x}As$ On GaAs(100)", Proceedings of MRS Fall 1990 symposium on "Evolution of Thin Film and Surface Microstructure", Boston, Mass., MRS Proceedings, 519, 202 (1991).

24. K.C. Rajkumar, P. Chen and A. Madhukar, "Reflection Electron Diffraction and Structural Behavior of GaAs/GaAs(111)B Grown via MBE", Proceedings of MRS Fall Meeting, Boston, Mass. Nov. 1990, MRS Symp. Proc. 208, 193 (1991).

25. R.M. Kapre, A. Madhukar and S. Guha, "Highly Strained GaAs/InGaAs/AlAs Resonant Tunneling Diodes with Simultaneously High Peak Current Densities and Peak-to-Valley Ratios at Room Temperature", App. Phys. Lett. 58, 2255 (1991).

26. K.Z. Hu, L. Chen, A. Madhukar, P. Chen, K.C. Rajkumar, K. Kaviani, Z. Karim, C. Kyriakakis and A.R. Tanguay, Jr., "High Contrast Ratio and Throughput Asymmetric Fabry-Perot Reflection Light Modulator Based on GaAs/InGaAs Multiple Quantum Wells" Appl. Phys. Lett. 59, 1108 (1991).

27. K.Z. Hu, L. Chen, A. Madhukar, P. Chen, C. Kyriakakis, Z. Karim, and A.R Tanguay, Jr., "An Inverted Cavity GaAs/InGaAs Asymmetric Fabry-Perot Reflection Modulator", Appl. Phys. Lett. 59, 1664 (1991).

28. Li Chen, KeZhong Hu, K.C. Rajkumar, S. Guha, R. Kapre and A. Madhukar, "Strained InGa/GaAs Multiple Quantum Wells Grown on Planar and Pre-Patterned GaAs(100) Substrates Via Molecular Beam Epitaxy: Applications to Light Modulators and Detectors", MRS Proc. 228,213 (1991).

29. K.Z. Hu, L. Chen, R. Kapre, K.C. Rajkumar, A. Madhukar, Z.Karim, C. Kyriakakis and A. Tanguay, Jr., "The Growth and Performance of Strained InGaAs/GaAs Multiple Quantum Well Based Asymmetric Fabry-Perot Reflection Modulators", IEEE/LEOS Topical Meeting on "Epitaxial Materials and In-Situ Processing for Optoelectronic Devices", July 29-31, 1991, Newport Beach, CA (pg.18).

30. K.Z. Hu, L. Chen, A. Madhukar, P. Chen, Q. Xie, K.C. Rajkumar, and K. Kaviani, "Growth, Behavior, and Applications of Strained GaInAs/AlGaAs Multiple Quantum Well Based Asymmetric Fabry-Perot Reflection Modulators", MRS Symp. Proc. 240, 615 (1992).

31. L. Chen, W. Chen, K.C. Rajkumar, K.Z. Hu, and A. Madhukar, "Observation of the Influence of Strain Induced Deep Level Defects on the Electroabsorption Characteristics of InGaAs/GaAs(100) Multiple Quantum Well Structures and Implications for Light Modulators", MRS Symp. Proc. 240, 621 (1992).

32. L. Chen, K.Z. Hu, R.M. Kapre and A. Madhukar, "High Contrast Ratio Self Electro-optic Devices Based on Inverted InGaAs/GaAs Asymmetric Fabry-Perot Modulator", App. Phys. Letts. 60, 422 (1992).

33. K.Z. Hu, L. Chen, K. Kaviani, P. Chen, and A. Madhukar, "All Optical Photonic Switches Using Integrated Inverted Asymmetric Fabry-Perot Modulators and Heterojunction Phototransistors", IEEE Photonics Technology Letters, 4, 263 (1992).

34. K.C. Rajkumar, K. Kaviani, J. Chen, P. Chen, and A. Madhukar, "Nanostructures on GaAs(111)B via Photolithography", App. Phys. Letts. 60, 850 (1992).

35. K. Kaviani, J. Chen, K.Z. Hu, L. Chen, and A. Madhukar, "Growth of High Quality Strained $Al_xGa_{1-x}As/In_{0.26}Ga_{0.74}As/Al_zGa_{1-z}As$ Quantum Wells and the Effect of Silicon Nitride Encapsulation and Rapid Thermal Annealing," Jour. Vac. Sc. Tech. B 10, 793 (1992).

36. D. H. Rich, K.C. Rajkumar, Li Chen, A. Madhukar and F.J. Grunthaner, "Defects in strained $In_{0.2}Ga_{0.8}As$/GaAs multiple quantum wells on patterned and unpatterned substrates: A near-infrared cathodoluminescence study", J. Vac. Sci. Technol.10, 1965 (1992).

37. D.H. Rich, K.C. Rajkumar, Li Chen, A. Madhukar and F.J. Grunthaner, "Near-infrared cathodoluminescence imaging of defect distributions in $In_{0.2}Ga_{0.8}As$/GaAs multiple quantum wells grown on prepatterned GaAs," Appl. Phys. Lett. 61, 222 (1992)

38. K.C. Rajkumar, K. Kaviani, J. Chen, P. Chen, A. Madhukar, and D.H. Rich, " *In-Situ* approach of three-dimensionally confined structures on patterned GaAs(111)B substrates," MRS Proc., 263, 163 (1992).

39. W. Chen, P. Chen, R. Viswanathn, A. Madhukar, J. Chen, K. Kaviani, Q. Xie, and K. Hu, "Physical and chemical effects of focused Ga-Ion Beam on GaAs (100)," MRS Symp. Proc. 268, 301 (1992).

40. K.C. Rajkumar, K. Kaviani, P. Chen, A. Madhukar, K. Rammohan and D.H. Rich, "One-step *in-situ* quantum dots via molecular beam epitaxy," J. Crystal Growth 127, 863 (1993)

41. A. Madhukar, K.C. Rajkumar, and P. Chen, "An *in-situ* approach to realization of three-dimensionally confined structures via substrate encoded size reducing epitaxy on nonplanar patterned substrates," Appl. Phys. Lett., 62, 1547 (1993).

42. W. Chen, P. Chen, A. Madhukar, R. Viswanathan, J. So, "Creation of 3D patterns in Si by focused Ga-Ion beam and anisotropic wet chemical etching," MRS Symp. Proc. 279 593(1993)

43. K. Kaviani, K. Hu, Q. Xie, A. Madhukar, " Realization of high performance doped channel MISFETs in highly strained AlGaAs/InGaAs/AlGaAs based quantum well", Jour. of Crystal Growth, 127, 68(1993).

44. K. Kaviani, L. Chen, K. Hu, Q. Xie, and A. Madhukar, " Effect of structural and chemical parameters on the optical properties of highly strained AlGaAs/InGaAs/AlGaAs quantum wells", J. Vac. Sci. Technol. B 11, 805(1993).

45. S. Guha and A. Madhukar, "An explanation for the directionality of interfacet migration during molecular beam epitaxical growth on patterned substrates", J. Appl. Phys. 73, 8662(1993).

46. K.C. Rajkumar, A. Madhukar, K. Rammohan, D H. Rich, P. Chen, and L. Chen, App. Phys. Lett. (Submitted)

47. K. C. Rajkumar, A. Madhukar, P. Chen, A. Konkar, L. Chen, K. Rammohan, and D. H. Rich (to be published).

III. CONFERENCE PRESENTATIONS

1. K.C. Rajkumar, P. Chen, and A. Madhukar, 20th ICPS Conference, Aug. 1990, Thessaloniki, Greece.

2. Li Chen, A. Madhukar, K.C. Rajkumar, K. Hu, and J.J. Jung, 20th ICPS Conference, Aug. 1990, Thessaloniki, Greece.

3. S. Guha, K.C. Rajkumar and A. Madhukar, 6th International MBE Conference, Aug. 1990, San Diego, CA.

4. Li Chen, K.C. Rajkumar, A. Madhukar, Wei Chen, S. Guha and K. Kaviani, 6th International MBE Conference, Aug. 1990, San Diego, CA.

5. S. Guha, A. Madhukar, R. Kapre and K.C. Rajkumar, MRS Fall 1990 Meeting, Boston, Mass.

6. P. Chen, K.C. Rajkumar, and A. Madhukar, PCSI 20 Conference, Long Beach, CA, Jan. 1991.

7. K.Z. Hu, L. Chen, R. Kapre, K.C. Rajkumar, A. Madhukar, Z. Karim, C. Kyriakakis, and A.R. Tanguay, Jr., "The Growth and Performance of Strained InGaAs/GaAs Multiple Quantum Well Based Asymmetric Fabry-Perot Reflection Modulators," IEEE-LEOS Topical Meeting, July 29 - 31, 1991 (Newport Beach, Ca).

8. K. Kaviani, J. Chen, K.Z. Hu, L. Chen, and A. Madhukar, "Growth of High Quality Strained $Al_xGa_{1-x}As/In_{0.26}Ga_{0.74}As/Al_zGa_{1-z}As$ Quantum Wells and the Effect of Silicon Nitride Encapsulation and Rapid Thermal Annealing," MBE Workshop (Austin, Texas) Sept. 16-19, 1991.

9. K.Z. Hu, L. Chen, A. Madhukar, P. Chen, Q. Xie, K.C. Rajkumar, and K. Kaviani, "Growth, Behavior, and Applications of Strained GaInAs/AlGaAs Multiple Quantum Well Based Asymmetric Fabry-Perot Reflection Modulators," MRS Fall Symp. Dec. 2-6, 1991 (Boston, Ma).

10. L. Chen, K.Z. Hu, K.C. Rajkumar, S. Guha, R. Kapre, and A. Madhukar, "Strained InGaAs/GaAs Multiple Quantum Wells Grown on Planar and Pre-Patterned GaAs(100) Substrates Via Molecular Beam Epitaxy: Applications to Light Modulators and Detectors," MRS Spring Symp. Proc., April 31-May 3, 1991 (Anaheim).

11. D.H. Rich, K.C. Rajkumar, L. Chen, A. Madhukar, T. George, J. Maserjian, F.J. Grunthaner, and A. Larsen, "Defects in Strained $In_{0.2}Ga_{0.8}As/GaAs$ Multiple Quantum Wells on Patterned and Unpatterned Substrates: A Near-Infrared Cathodoluminescence Study," PCSI 21 (Death Valley, Ca) Jan. 1992.

12. K.C. Rajkukmar, K. Kaviani, J. Chen, P. Chen, A. Madhukar, and D.H. Rich, "One-step *In-situ* Quantum dots via Molecular Beam Epitaxy," MRS Spring Symp. Proc., April 1992 (San Francisco, CA)

13. W. Chen, R. Viswanathan, P. Chen, A. Madhukar, K. Kaviani, Q. Xie, J. Chen, and K. Hu, "Physical and Chemical Effects of Focused Ga-Ion Beam on Semiconductor Materials and Their Impact on the Subsequent Overgrowth," MRS Spring Symp. Proc., April 1992 (San Francisco, CA)

14. W. Chen, P. Chen, A. Madhukar, R. Viswanathan, and J. So, "Creation of 3D Patterns in Si by Focused Ga-Ion Beam and Anistropic Wet Chemical Etching," MRS Fall Symp. Proc., December 1992 (Boston, MA)

IV. PERSONNEL

: Graduate Students

1. Supratik Guha, (Ph.D. Jan. 1991)
2. Ravindra M. Kapre, (Ph.D. May 1991)
3. Li Chen, (Ph.D. May 1993)
4. Kian Kaviani, (Ph.D. Apr. 1993)
5. Kezhong Hu (Ph.D. expected Sep. 1993)
6. K.C. Rajkumar, (Ph.D. expected Dec. 1993)
7. Wei Chen, (Ph.D. expected Dec. 1993)
8. Atul Konkar, (Ph.D. expected 1996)
9. Qianghua Xie, (Ph.D. expected 1995)

: Post-Doctoral Fellows

1. Dr. Ping Chen (Feb. 1990 - present)
2. Dr. R. Kapre (Jun. 1991 - Aug. 1991)
3. Dr. Li Chen (May 1993 - present)